A specialized histone H1 variant is required for adaptive responses to complex abiotic stress and related DNA methylation in Arabidopsis

Rutowicz, Kinga ; Puzio, Marcin ; Halibart-Puzio, Joanna ; et al

Abstract: Linker (H1) histones play critical roles in chromatin compaction in higher eukaryotes. They are also the most variable of the histones, with numerous nonallelic variants cooccurring in the same cell. Plants contain a distinct subclass of minor H1 variants that are induced by drought and abscisic acid and have been implicated in mediating adaptive responses to stress. However, how these variants facilitate adaptation remains poorly understood. Here, we show that the single Arabidopsis (Arabidopsis thaliana) stress-inducible variant H1.3 occurs in plants in two separate and most likely autonomous pools: a constitutive guard cell-specific pool and a facultative environmentally controlled pool localized in other tissues. Physiological and transcriptomic analyses of h1.3 null mutants demonstrate that H1.3 is required for both proper stomatal functioning under normal growth conditions and adaptive developmental responses to combined light and water deficiency. Using fluorescence recovery after photobleaching analysis, we show that H1.3 has superfast chromatin dynamics, and in contrast to the main Arabidopsis H1 variants H1.1 and H1.2, it has no stable bound fraction. The results of global occupancy studies demonstrate that, while H1.3 has the same overall binding properties as the main H1 variants, including predominant heterochromatin localization, it differs from them in its preferences for chromatin regions with epigenetic signatures of active and repressed transcription. We also show that H1.3 is required for a substantial part of DNA methylation associated with environmental stress, suggesting that the likely mechanism underlying H1.3 function may be the facilitation of chromatin accessibility by direct competition with the main H1 variants.

DOI: https://doi.org/10.1104/pp.15.00493

Running title: Linker histones in plant adaptation to stress

Andrzej Jerzmanowski

Institute of Biochemistry and Biophysics, Polish Academy of Sciences

Pawinskiego 5a

02-106 Warsaw

Poland

Telephone number: +48 22 5925704

andyj@ibb.waw.pl

Research Area: Genes, development and evolution

Secondary Research Area: Chromatin and epigenetics

A specialized histone H1 variant is required for adaptive responses to complex abiotic stress and related DNA methylation in Arabidopsis

Kinga Rutowicz[1], Marcin Puzio[2], Joanna Halibart-Puzio[1,3], Maciej Lirski[1], Maciej Kotliński[1,2], Magdalena A Kroteń[4], Lukasz Knizewski[5], Bartosz Lange[2], Anna Muszewska[1,5], Katarzyna Śniegowska-Świerk[6], Janusz Kościelniak[6], Roksana Iwanicka-Nowicka[1,2], Krisztián Buza[7], Franciszek Janowiak[8], Katarzyna Żmuda[6], Indrek Jõesaar[9], Katarzyna Laskowska-Kaszub[2], Anna Fogtman[1], Hannes Kollist[9], Piotr Zielenkiewicz[1], Jerzy Tiuryn[7], Paweł Siedlecki[1,2], Szymon Swiezewski[1], Krzysztof Ginalski[5], Marta Koblowska[1,2], Rafał Archacki[2], Bartek Wilczynski[7], Marcin Rapacz[6] and Andrzej Jerzmanowski[1,2]*

[1]Institute of Biochemistry and Biophysics, Polish Academy of Sciences (Pawinskiego 5a, 02-106 Warsaw, Poland);

[2]Laboratory of Systems Biology, University of Warsaw (Pawinskiego 5a, 02-106 Warsaw, Poland);

[3]Institute of Plant Physiology, University of Rzeszów, (Werynia 502, 36-100 Kolbuszowa)

[4]College of Inter-Faculty Individual Studies in Mathematics and Natural Sciences, University of Warsaw (Żwirki i Wigury 93, 02-089 Warsaw, Poland).

[5]Laboratory of Bioinformatics and Systems Biology, CeNT, University of Warsaw (S. Banacha 2c, 02-097 Warsaw, Poland).

[6]Department of Plant Physiology, University of Agriculture in Cracow (Podłużna 3, 30-239 Cracow, Poland).

[7]Institute of Informatics, University of Warsaw (Banacha 2, 02-097 Warsaw).

[8]Institute of Plant Physiology, Polish Academy of Sciences (Niezapominajek 21, 30-239 Cracow).

[9]Institute of Technology, University of Tartu (Nooruse 1, 50411, Tartu, Tartumaa, Estonia).

*Correspondence to: andyj@ibb.waw.pl

Summary:

An environmentally controlled linker histone facilitates chromatin changes associated with the response to complex abiotic stress in Arabidopsis

Financial sources:

This research was funded by the Institute of Biochemistry and Biophysics - Polish Academy of Sciences and the University of Warsaw; grants from the European Cooperation in Science and Technology [MNiSW 212/N-COST/2008/0] to A.J.; Ministry of Science and Higher Education [MNiSW/PO4A/03928] to A.J.; [MNiSW/NN301/269237] to K.R. and S.S.; [MNiSW/NN301/033234] to M.P., [MNiSW/NN301/201539] to J.H.P., [PBZ-MNiI-2/1/2005] and [MNiSW/NN301/469138] to M.K.; Foundation for Polish Science [TEAM/2010-6], National Science Centre [2011/02/A/NZ2/00014] and National Centre for Research and Development (PBS1/A9/16/2012) to K.G.; University of Agriculture in Cracow [DS3113/KFR/2012-14] to M.R., K.Ś.Ś., J.K. and K.Ż.; Estonian Research Council (IUT2–21) and European Regional Fund (CoE Environ) grants to H.K.

Present address(es) of authors if different from heading:

Kinga Rutowicz

Institute of Plant Biology, University of Zurich, Zollikerstrasse 107, CH-8008 Zurich, Switzerland

Katarzyna Laskowska-Kaszub

Laboratory of Preclinical Testing of Higher Standard, Nencki Institute of Experimental Biology, Pasteura 3, 02-093 Warsaw

Corresponding author with e-mail address:

Andrzej Jerzmanowski, andyj@ibb.waw.pl

Abstract

Linker (H1) histones play critical roles in chromatin compaction in higher eukaryotes. They are also the most variable of the histones, with numerous non-allelic variants co-occurring in the same cell. Plants contain a distinct subclass of minor H1 variants that are induced by drought and ABA, and have been implicated in mediating adaptive responses to stress. However, how these variants facilitate adaptation remains poorly understood. Here we show that the single *Arabidopsis thaliana* stress-inducible variant H1.3 occurs in plants in two separate and most likely autonomous pools: a constitutive guard cell-specific pool and a facultative environmentally controlled pool localized in other tissues. Physiological and transcriptomic analyses of *h1.3* null mutants demonstrate that H1.3 is required for both proper stomatal functioning under normal growth conditions and adaptive developmental responses to combined light and water deficiency. Using FRAP analysis we show that H1.3 has superfast chromatin dynamics, and in contrast to the main Arabidopsis H1 variants H1.1 and H1.2, it has no stable bound fraction. The results of global occupancy studies demonstrate that while H1.3 has the same overall binding properties as the main H1 variants, including predominant heterochromatin localization, it differs from them in its preferences for chromatin regions with epigenetic signatures of active and repressed transcription. We also show that H1.3 is required for a substantial part of DNA methylation associated with environmental stress, suggesting that the likely mechanism underlying H1.3 function may be the facilitation of chromatin accessibility by direct competition with the main H1 variants.

1

Introduction

Linker (H1) histones are conserved and ubiquitous structural components of eukaryotic chromatin required for the stabilization of higher-order chromatin structure, and are generally thought to restrict DNA accessibility. Interestingly, despite their architectural role, H1 histones were shown to be highly mobile and continuously exchanging among chromatin binding sites (Raghuram et al., 2009). They are also the most variable of the histones, with numerous non-allelic variants co-existing in the same cell. In vertebrates, several evolutionarily conserved subfamilies of H1 can be distinguished (Talbert et al., 2012), and appear to play both redundant and specific roles during development and cellular differentiation (McBryant et al., 2010). There is accumulating evidence that in animals, regulation of the proportions of H1 variants with different dynamic behavior in chromatin is involved in controlling the accessibility of DNA to *trans*-acting factors (Jullien et al., 2010, Shahhoseini et al., 2010, Perez-Montero et al., 2013, Zhang et al., 2012a, Christophorou et al., 2014).

Epigenetic mechanisms, including DNA and histone modifications and active nucleosome remodeling, are major players in translating signals about environmental perturbations into adaptive responses at the transcriptional level (Smith and Workman, 2012, Kinoshita and Seki, 2014). In the last decade, considerable progress has been made in understanding the function of H1 in shaping chromatin epigenetic signatures (Harshman et al., 2013). Importantly, in both plants and animals, H1 histones are involved in maintaining the pattern of DNA methylation (Wierzbicki and Jerzmanowski, 2005, Fan et al., 2005, Zemach et al., 2013). As suggested by these studies, H1 is most likely a major regulator of the accessibility of chromatin to DNA methyltransferases. It was also shown to be involved in chromatin reprogramming during the somatic-to-reproductive cell fate transition in Arabidopsis (She et al., 2013).

Plant H1s can be divided into ubiquitously and stably expressed major (main) variants and stress-inducible minor variants (Talbert et al., 2012, Jerzmanowski et al., 2000). The minor variants subfamily is evolutionarily conserved and ancient since it appeared before the split into mono- and dicotyledonous plants (Jerzmanowski et al., 2000). The model plant *Arabidopsis thaliana* has three non-allelic H1s: the highly similar major variants H1.1 and H1.2, and a single stress-inducible minor variant H1.3 (Jerzmanowski et al., 2000).The occurrence of the stress-inducible linker histones was discovered when an *H1-D* gene in tomato *Lycopersicon pennellii*

was identified and shown to be strongly induced by drought stress and abscisic acid (ABA) (Cohen and Bray, 1990, Cohen et al., 1991, Plant et al., 1991, Wei and O'Connell, 1996). Close homologs were subsequently identified in other plant species (e.g. Arabidopsis, tobacco) and shown to be induced by similar conditions (Ascenzi and Gantt, 1997, Przewloka et al., 2002).

Importantly, immunostaining of whole nuclei with specific antibodies showed that the distribution of H1.3 differed from that of H1.1 and H1.2 (which was identical), suggesting that H1.3 binds to different genomic regions compared with the main H1 variants (Ascenzi and Gantt, 1999b). Arabidopsis, tomato and tobacco plants with down-regulation of the stress-inducible linker histone variant do not show defects in development and global chromatin organization under normal conditions (Scippa et al., 2004, Ascenzi and Gantt, 1999a, Scippa et al., 2000, Przewloka et al., 2002), suggesting that this group of linker histones has no major role in the basal functions of plant development nor in chromatin structure. However, the tomato *Lycopersicon esculetum* homolog H1-S has been implicated in maintaining the water status during a specific window in drought treatment. Transgenic tomato plants with down-regulated H1-S showed increased stomatal conductance, transpiration and photosynthetic rate compared with wild-type plants, consistent with a role for this protein in regulating stomatal function (Scippa et al., 2004).

In contrast to *Lycopersicon esculetum*, the depletion of stress-inducible H1 variants in *Lycopersicon pennellii* and in Arabidopsis was not accompanied by observable changes in the drought response (Wei and O'Connell, 1996, Ascenzi and Gantt, 1999a), so the biological role of these proteins remains unclear. Nevertheless, the sequence homology of the drought stress inducible variants, and the fact that unlike other known histone genes they can be regulated by environmental factors, lend support to the suggestion that these H1 variants may play some special role in the regulation of gene expression.

Here, we used previously unavailable molecular and genetic tools to address the following questions: 1. How are Arabidopsis linker histones distributed in the plant under normal and stress conditions? 2. Are there environmental conditions under which H1.3 becomes a limiting factor to adaptive responses? 3. Where and how does H1.3 bind in the genome under normal and stress conditions? 4. Is there a functional link between its binding properties and cellular reprograming during physiological responses to stress?

We show that prolonged growth in low light leads to robust induction of H1.3 protein, which enables in depth characterization of the entire complement of linker histones in Arabidopsis under both normal and stress conditions, including their *in vivo* binding properties and global occupancy profiles along chromosomes. We further establish that stress-inducible H1.3 is represented in Arabidopsis by two independent pools: one constitutive, confined to guard cells, and the other facultative, occurring in other tissues, which is controlled by environmental cues. Furthermore, we show that H1.3 is required for both stomatal functioning under normal growth conditions and for adaptive developmental responses to complex environmental stress of combined light and water deficiency. In addition, the depletion of H1.3 abolishes a substantial part of stress-related DNA methylation. Taken together, our findings suggest that H1.3 mediates adaptive responses to complex environmental stress *via* global alteration of chromatin properties, which favors reprogramming of the epigenetic landscape and gene expression.

Results

Prolonged growth of Arabidopsis under a low-light regime leads to the robust induction of H1.3 protein in most tissues

The limited repertoire of linker histone variants makes Arabidopsis an ideal model to study the possible adaptive role of the 'stress-inducible' H1s in plants. To assess the distribution of H1 variants in a tissue-specific manner, we used transgenic lines expressing H1-GFP fusion proteins under the control of their native promoters. H1.1 and H1.2 fused to GFP were detected in all vegetative tissues and organs, while the H1.3-GFP was observed almost exclusively in guard cells (Fig. 1A). This is consistent with the findings of an earlier study using transcriptional fusions (Ascenzi and Gantt, 1999a), and with transcriptome analyses showing that *H1.3* is one of the most highly expressed transcripts in guard cells (Leonhardt et al., 2004).

When we compared *H1.3* expression in plants subjected to different environmental stresses (not shown), we found that reduced light intensity during the day induced a remarkable global increase in H1.3-GFP in shoot and root tissues (Fig. 1A). Under these conditions, H1.3 appeared co-expressed in the same cells as the H1.1 and H1.2 variants (Fig. 1A). The low light conditions we used were reported previously to cause reduction in chromatin compaction (van Zanten et al., 2010). At the transcript level, *H1.3* showed an increase of 10- to 35-fold from its basal level in non-induced plants, depending on the age of the plant and probably other uncontrolled factors

(Fig. 1B, Supplemental Fig. S1A). This is consistent with the results of genome-wide expression profiling experiments, including data from dedicated large-scale projects, and online tools like GENEVESTIGATOR (Zimmermann et al., 2004) and AtGeneExpress (Schmid et al., 2005, Kilian et al., 2007), showing that the expression of *H1.3* is characterized by exceptionally high-amplitude fluctuations in roots, stems and leaves depending on growth conditions, developmental stage and differentiation level (Supplemental Fig. S2). The induction of *H1.3* was equally effective in both the Ler and Col-0 ecotypes (Supplemental Fig. S1A,B). Importantly, the effect of low light on the expression of *H1.3* was significantly stronger than that of complete darkness (Supplemental Fig. S1C). The systemic induction of H1.3-GFP required 3-4 days of low light. Moreover, within 1-2 days after restoring standard light conditions, *H1.3* expression, as determined by transcript abundance, had returned to its normal low level (Fig. 1C).

The *H1.3* transcript is up-regulated in response to ABA treatment (AtGeneExpress, Fig. S1D). To determine whether *H1.3* induction under low light depends on the ABA signaling pathway, we examined the level of *H1.3* mRNA in the ABA-deficient *aba1* mutant grown in low light. On average, *H1.3* transcript levels in the mutant were 5-fold lower than those in wild-type plants (Fig. 1D), indicating that *H1.3* expression strongly depends on the ABA signaling pathway. This is consistent with the presence of ABA-Responsive Elements (ABRE) close to the transcription start site in the *H1.3* promoter (Supplemental Fig. S3) (Fujita et al., 2011) (Gomez-Porras et al., 2007, Berendzen et al., 2006). Interestingly, an autonomous ABA biosynthesis pathway in guard cells was recently discovered (Bauer et al., 2013), and this could account for the stable occurrence of H1.3 in these highly specialized cells. In contrast to ABA-deficiency, the absence of the main photoreceptors (*PhyA/PhyB, Cry1/Cry2*) not only did not inhibit, but slightly enhanced the induction of *H1.3* by low light (Supplemental Fig. S1E), suggesting their possible negative role in low light-induced *H1.3* expression in wild-type plants. Interestingly, H1.3 was recently shown to belong to a narrow group of 39 genes comprising a core response module with a critical role in retrograde plastidial-to-nucleus signaling (Glasser et al., 2014). Thus, its up-regulation could be the result of complex secondary effects (including, but not restricted to an increase in ABA) of the change in redox levels due to reduced photosynthetic activity (Pfalz et al., 2012). This is consistent with the relatively small role in *H1.3* regulation of the major photoreceptors, which are known to play only a minor function in retrograde signaling (Fey et al., 2005, Lepisto et al., 2012).

Lack of H1.3 affects stomatal functions and development

In order to assess the role of H1.3 in Arabidopsis physiological responses, we used *h1.3* null mutants (Supplemental Fig. S4) in parallel with their sibling wild-type plants. To examine plant responses to conditions closely resembling those occurring naturally, where light fluence on a moderately cloudy summer day is in the range of 350-450 µmol m^{-2} s^{-1}, we studied plants grown in 400 µmol m^{-2} s^{-1} rather than 150 µmol m^{-2} s^{-1} light fluence (standard for laboratory experiments with Arabidopsis). We also assumed that any differences between control and low light conditions would be observed more readily when the change in light fluence was an increase rather than a decrease. Using the H1.3-GFP line, we first confirmed that the H1.3 protein was not induced by the raised light fluence and was only visible in guard cells, similar to Figure 1. Wild-type and *h1.3* plants grown under high-light conditions were similar in size (Supplemental Tables S1 and S2), but the mutant plants were characterized by a reduced CO_2 assimilation rate per plant (Fig. 2A) and a decreased stomatal density in young leaves, especially in the upper epidermis (Fig. 2B, Supplemental Fig. S5A). This suggested a role for H1.3, not only in the regulation of stomatal functioning, in accordance with an earlier report (Scippa et al., 2004), but, unexpectedly, also in their development. To determine whether the above differences were reflected at the level of gene transcription, we compared the transcriptomic profiles of wild-type and *h1.3* plants in control conditions using AGRONOMICS microarrays and found that nearly 10% of genes were differentially expressed in the mutant, although most of the observed changes in gene expression were moderate (Supplemental Dataset S1). Interestingly, the proportion of genes showing altered expression (categorized as differentially expressed if fold change [Fch]>1.5 and p-value [p]<0.05) due to H1.3 depletion was highest (almost 30%) among those reported to be preferentially expressed in guard cells (Fig. 2C). Moreover, the depletion of H1.3 significantly affected the expression of key genes involved in stomatal development, including *SPCH*, *MUTE*, *FAMA*, *ERf/TMM* and *MKK9*, encoding a mitogen activated protein kinase (Fig. 2D). These genes are not expressed in mature guard cells, but in different developmental phases of the stomatal lineage, including the meristemoid cell, a stem-cell-like stomatal precursor (Lau and Bergmann, 2012). Most of these genes, with the exception of *MKK9* that was up-regulated, were down-regulated in parallel with the decrease in stomatal density in the *h1.3* mutant (Fig. 2B). Interestingly, the loss-of-function *spch* mutants lacked stomata on the leaf epidermal surfaces and died early (MacAlister et al., 2007). However, in contrast to the null

mutant, the expression of *SPCH* in the *h1.3* mutant, albeit low, was clearly detectable. There is no proof of a linear relationship between *SPCH* transcript and protein levels; on the contrary, Arabidopsis was shown to have an efficient system controlling SPCH abundance (Kumari et al., 2014), highlighting the importance of posttranscriptional regulation in this case. It is thus plausible that the level of the *SPCH* transcript detected in the *h1.3* mutant was still sufficient for the induction of stomata, although at decreased density, as shown in Fig. 2B.

After normalization of expression values against the number of stomata, the overall pattern was similar to that before normalization: the expression of *ER*, *TMM* and *SPCH* was lower and that of *MKK9* higher in the *h1.3* mutant than in the wild-type. However, there was no difference between the mutant and wild-type plants in the expression of *FAMA* and *MUTE*, suggesting that the reduced expression of these two genes may result from lowering the number of stomata (Supplemental Fig. S5B).

Taken together, our results are consistent with the notion that H1.3 acts as a regulator of stomatal functions. Further studies are required to determine whether the significant changes in the transcription of key genes regulating stomatal development from precursor cells, observed in the *h1.3* mutant, are due to the direct effect of H1.3 on these genes or are an indirect effect of impaired stomatal physiology in early development that leads to altered stomatal development in young leaves.

H1.3 is required for the reduction of Arabidopsis growth in response to combined low-light/drought treatment

Stress-inducible H1s are up-regulated by drought (Ascenzi and Gantt, 1997, Scippa et al., 2000) and the effects of RNAi-mediated down-regulation of a tomato homolog of H1.3 suggested that they may promote plant sensitivity to water stress (Scippa et al., 2004). A comparison of the efficiency of limited drought and low light in inducing *H1.3* expression showed that 17 days of water limitation was as effective as the same period of low light in inducing the accumulation of *H1.3* mRNA. Surprisingly, levels of this transcript increased synergistically when the two stresses were combined (Fig. 3A), suggesting that plants responded to this combination of stresses in a synergistic manner. All plants were subjected to soil water

deficit under both low- and high-fluence light conditions, and different morphological and physiological parameters were assessed (Fig. 3B-D; Supplemental Tables S1 and S2).

The normal reaction of Arabidopsis to water limitation is growth retardation, resulting mainly from decreased biomass accumulation after stomatal closure under mild drought conditions and more rapid generative development (Chaves et al., 2009). A graph of the average quantitative phenotype confirmed our earlier observation that wild-type and *h1.3* null plants were morphologically indistinguishable when grown in control conditions (Fig. 3D). However, in combined low light/drought, the *h1.3* plants had a higher leaf number and an increased dry and fresh weight compared with wild-type plants, irrespective of the growth stage at which they were subjected to drought (Fig. 3D, Supplemental Fig. S6-S7; Supplemental Tables S1 and S2). Stem formation and flowering under low light/drought stress occurred more slowly in *h1.3* plants than in wild-type plants. The *h1.3* plants showed not only an increased growth rate compared to wild-type plants, but also a higher net photosynthetic rate (Supplemental Tables S1, S2) and lower relative water content (RWC) in their leaves (Fig. 3B). Interestingly, the water content per dry weight (WC) in drought was similar in the wild-type and *h1.3* plants (Fig. 3C). This suggested that the observed changes in RWC resulted from differences in the accumulation of osmolytes in the leaf cells. The stomatal density (SD) in the lower epidermis of *h1.3* plants decreased only 2-fold in low light/drought conditions, compared to a 4-5-fold decrease in wild-type plants. In the *h1.3* mutant, the SD, while lower in control conditions, was higher under low light/drought than in WT plants (Supplemental Fig. S5), which is indicative of the decreased ability of *h1.3* plants to adjust stomatal biogenesis to environmental conditions (Fig. 2). While it is likely that differences in the photosynthetic rate and RWC caused by low light/drought were mostly due to changes in stomatal activity non-stomatal factors cannot be ruled out. The differences in the growth retardation effect of low light/drought (Fig. 3D) could be due to changes in the leaf ABA content; however, we found similar ABA levels in *h1.3* and wild-type plants (Supplemental Fig. S8). This points to differences in downstream ABA targets as the possible cause of the observed phenotypes. Importantly, all of the physiological and developmental effects of the *h1.3* mutation in plants under stress described above, were not observed in mutant plants complemented with H1.3-GFP, which reacted similarly to the wild-type (Fig. 3D, Supplemental Fig. S7; Supplemental Tables S1, S2). In natural conditions, the inability to restrict growth and photosynthetic rate under prolonged low light/drought stress confers only a very short term

advantage. In the longer term, it obviously impairs a common adaptive strategy of plants under such conditions (i.e. restriction of metabolism and growth, leading to delayed reproduction), aimed at minimizing the loss in fitness. To better understand the molecular basis of the observed *h1.3* phenotype, we performed global transcriptome profiling. Exposure of wild-type Arabidopsis to mild drought and low light conditions induced strong transcriptional reprogramming. The genes that were most affected included those classified as responsive to stress, hormones and environmental stimuli, and those connected with lipid and cell wall functions (Supplemental Dataset S2, AgriGO (Du et al., 2010)). Importantly, the response of *h1.3* mutants during stress differed considerably from that of wild-type plants (Fig. 3E; Supplemental Datasets S2,S3). In response to the imposed environmental changes, wild-type plants showed altered expression of about 705 genes (Fch≥2; p-value<0.05), whereas the transcript levels of twice that number of genes (1412) were changed in the *h1.3* mutant, with only 23% of these in common with the wild-type (Fig. 3E). When interpreting these differences it should be remembered that under control conditions, wild-type and *h1.3* plants differ in their expression of about 10% of all genes, many of which play a critical role in stomatal biogenesis and function (Supplemental Dataset S2). It is possible that this major primary difference could lead to amplified secondary differences under stress conditions.

Comparison of the transcriptomic profiles of wild-type and *h1.3* mutant plants grown under stress conditions revealed that in the absence of H1.3, 70% of the affected transcripts were down-regulated (Fch>1.5; p-value<0.05), and this value increased to 82% for a fold change of >3, while in control conditions the equivalent proportions of down-regulated transcripts were 58% for a fold change of >1.5 and 53% for a fold change of >3 (Supplemental Datasets S1, S4). This suggests that under conditions of stress, H1.3 acts mainly as a positive rather than a negative regulator of gene transcription.

H1.3 binds chromatin with considerably higher dynamics than the main H1 variants

In guard cells of non-stressed plants H1.1, H1.2 and H1.3 showed different mobility, with half-time recoveries ($T_{1/2}$) of 6.8, 16.8 and 3.4 sec, and stable bound pools of 28%, 14% and 3%, respectively. Interestingly, the characteristics of H1.2 resembled those of H2B ($T_{1/2}$ – 14.8 sec,

78% stable pool). These data showed that H1.3 is the most dynamic variant and probably occurs as a pool of rapidly diffusing molecules. (Fig.4; Supplemental Videos S1-S3).

We next compared H1 mobilities in the nuclei of root, hypocotyl and root meristem cells under control and low light growth conditions. H1.2 showed the lowest mobility in all analyzed tissues ($T_{1/2}$ of ~ 22 sec), indicative of the strongest interaction with chromatin. The low light-induced H1.3 consistently showed the highest mobility ($T_{1/2}$ of ~ 2-3 sec). The binding properties of H1.1 ($T_{1/2}$ of 6.2-16.2 sec) were more similar to H1.2 than to H1.3. In all three analyzed organs, the recovery of H1.2 was on average 30% faster in low light than in control conditions, which is consistent with its weaker interaction with chromatin after prolonged low light stress (Table 1). Moreover, the faster overall exchange of H1.2 in low light was mostly due to a significant increase in recovery during the first few seconds after photobleaching (not shown), which is indicative of an increased soluble or loosely bound pool in this initial phase (Phair et al., 2004). The mobility of H1.1 in low light changed to a lesser extent (9-16%) and increased only in root and meristem, whereas it decreased in hypocotyl (Table 1). The observed differences in histone mobilities among tissues, as measured by FRAP, are characteristic of cell differentiation and development in Arabidopsis and are probably due to changes in the global chromatin states (Rosa et al., 2014).

To summarize, we have demonstrated that H1.3 has no stable bound pool in the nucleus and exchanges in chromatin extremely rapidly. These properties may be caused by conserved amino acid replacements in the H1.3 GH1 binding sites S1 and S2, as well as the shortening of its C-terminal domain (CTD) (Supplemental Fig. S22). Interestingly, the appearance in evolution of stress-inducible H1s seems to coincide with the onset of angiosperms (Supplemental Figs. S12, S13 and S14).

Mapping the genome-wide distribution of H1 variants reveals differences in their preferences for epigenetic marks of active and repressive chromatin

The differences in the GH1 binding sites and CTD, and *in vivo* chromatin dynamics between the main linker histone variants and H1.3 prompted us to ask whether these two types of H1 also differ in their chromatin localization preferences. We used our H1-GFP tagged lines and ChIP-on-chip technology to analyze the distribution of all three H1 variants in Arabidopsis

plants grown in low light or in control conditions. Initially, we looked at overall patterns of H1 distribution among different types of sequences. Both the main and stress-inducible H1s were generally depleted in introns and 5'UTRs compared to exons, 3'UTRs and transposons (Fig. 5A, Supplemental Fig. S15). Interestingly, the magnitude of the enrichment compared to the total genome signal of the stress-inducible H1.3 to the main variants was markedly decreased on transposons compared with total genic regions or exons and 3'UTRs. (Fig. 5A, Supplemental Fig. S15).

Next, we analyzed the qualitative profiles of the main H1 variants and the core histone H3 along the chromosomes of Arabidopsis grown in control and low light conditions, and compared these with the H1.3 profile after its induction by low light. All three H1 variants were found to be enriched in pericentromeric regions (resembling the distribution pattern of heterochromatic transposons (Lippman et al., 2004)), but not in the central region of the centromere, where the signal for the core histone H3 was close to its maximum level (Supplemental Fig. S16). Importantly, while the intensity profiles for H1.1 and H1.2 along chromosomes were strongly correlated, independently of the growth conditions (Pearson's r: 0.97), the profile for H1.3 after its induction by low light was notably less correlated with those of the main variants (Pearson's r: 0.81 and 0.74, respectively). This suggests that despite their likely similar specificity for nucleosomal sites, the chromosome-wide occupancy of the main linker histone variants and H1.3 may be governed by different preferences for some additional feature(s) of these sites. This is consistent with an earlier report demonstrating that while H1.1 and H1.2 antibodies decorate nuclei in patterns very similar to DAPI staining, antibodies raised against H1.3 bind to chromatin in a diffuse pattern distinct from DAPI staining (Ascenzi and Gantt, 1999b).

The relative abundance of the main H1 variants was higher on heterochromatic compared to euchromatic transposons (Fig. 5B), resembling the preferences reported for mammalian somatic H1s (Cao et al., 2013, Izzo et al., 2013). In contrast, the abundance of low light-induced H1.3 appeared similar on the two transposon types (Fig. 5B). Interestingly, low light treatment led to a decreased relative abundance of H1.1 and H1.2 on the 5' and 3' ends of both heterochromatic and euchromatic transposons. Together, these characteristics are consistent with the possibility that while H1.3 generally competes with the main H1 variants for the same binding sites, its effects may be more pronounced in a specific subset of these sites.

We next compared the distribution of the nucleosomal core histone H3 and the H1 variants on genes with different transcriptional activity (Fig. 6). H3 mapping showed a typical well-positioned +1 nucleosome at the right border of the 5' nucleosome depleted region (NDR), coinciding approximately with the transcription start site (TSS). In accordance with data for other organisms (Jiang and Pugh, 2009), this pattern was most distinct for Arabidopsis genes with the highest transcriptional activity. The signals for all three H1 variants showed identical profiles, consistent with their ability to bind to the same sites. Interestingly, the inverse correlation between occupancy by H1 and the level of gene expression was weaker for H1.3 than for H1.1 and H1.2, suggesting that the presence of the former is less associated with actual transcriptional activity. While H3 was depleted in 5' and 3' NDRs and remained at a relatively stable level throughout gene bodies, the H1s were depleted at the -1 nucleosome and then rose steadily through the 5' NDR towards the +1 nucleosome, followed by an immediate downstream dip. This was followed by a steady increase in occupancy towards the 3' end, with a sharp decrease at the 3'NDR. Interestingly, the pattern of H1 binding was distinct from that of H3 in all analyzed groups of genes. The peak of H1 around the TSS and the neighboring upstream dip appeared slightly shifted in the 5' direction in relation to the H3 peak and the 5' NDR. The resolution of our data is not sufficient to establish whether this could be due to distinct DNA binding positions of H1 and H3: with H1 binding to linker DNA upstream of H3. In addition, the gene bodies (especially in highly expressed H3K4me3-marked genes) were not evenly covered by the H1 ChIP signal, suggesting that not all nucleosomes within the gene contain H1 at the same time. Moreover, nucleosomes close to the 5' ends of active genes were more often depleted in H1 than those at the 3' ends. The increasing H1 occupancy towards the 3' end of genes seems to be specific for plants, since no such feature was reported for human or Drosophila H1s (Braunschweig et al., 2009, Izzo et al., 2013). The question of whether this is related to transcription elongation and/or termination requires further investigation.

Importantly, apart from the inverse relationship between H1.3 binding and the level of gene expression, we detected no qualitative differences among the H1 variants in their patterns of binding along genes in both control and low light conditions, suggesting that the functions of H1.3 depend largely on its competition with the main H1s for the same binding sites (Fig. 5).

To identify the possible underlying causes of H1.3 chromatin binding site preferences, we analyzed the distribution of H1s in low light in relation to the known locations of H3K4me3 and

H3K9me2 methylation marks (Luo et al., 2012, Moissiard et al., 2012). In normal growth conditions, over 16,500 Arabidopsis genes were reported as H3K4me3-tagged, and over 3300 TEs and genes as H3K9me2-tagged (Zhou et al., 2010, van Dijk et al., 2010). Importantly, in both Arabidopsis and rice most of these genes were shown to remain tagged under stress conditions, including drought and decreased light (Zong et al., 2013, van Dijk et al., 2010, Guo et al., 2008). In accordance with their preferred localization in heterochromatin, all three H1 variants were negatively correlated with H3K4me3, an epigenetic mark associated with active chromatin. However, compared to H1.1 and H1.2, H1.3 was clearly less strongly anti-correlated with high levels of H3K4me3 (Fig. 7A), and unlike H1.1 and H1.2, the occupancy of H1.3 at both the 5' and 3' ends of genes marked with H3K4me3 was highest on those with the highest level of this modification (Fig. 7B, Supplemental Fig. S17). In contrast, its occupancy on genes marked with H3K9me2 was lowest on those with the highest level of this mark. (Fig. 7C, Supplemental Fig. S18). Thus, while it is evident from Fig. 6A that globally, most H1.3 is localized in heterochromatin, as expected for H1 histones, it seems to have an increased potential, compared to the main variants, to bind to sites enriched in epigenetic signatures of active chromatin. Together, our global mapping showed that the overall mode of binding is conserved between the main and stress-inducible H1 variants, indicating the potential for genome-wide competition. While localized mostly in heterochromatin, the members of these two subclasses seem to differ in their preferences for epigenetic signatures of active and inactive chromatin. In contrast to the main variants, the stress-inducible H1.3 shows a greater capability to associate with chromatin enriched in H3K4me3-marked genes.

H1.3 affects the level and targeting of stress-dependent DNA methylation

In both plants (Wierzbicki and Jerzmanowski, 2005, Zemach et al., 2013) and animals (Fan et al., 2005, Yang et al., 2013) H1 has been shown to be involved in establishing and maintaining patterns of DNA methylation. It was recently reported that the main Arabidopsis H1 variants H1.1 and H1.2 restrict the access of methyltransferases to nucleosomal DNA and that the ATP-dependent nucleosome remodeler DDM1 (Decrease of DNA Methylation 1) (Jeddeloh et al., 1998, Brzeski and Jerzmanowski, 2003) plays a major role in overcoming this restriction and enabling the occurrence and maintenance of DNA methylation, especially within

heterochromatin transposable elements (TEs) (Zemach et al., 2013). In order to assess the potential contribution of the stress-inducible H1.3 variant to these changes under normal growth conditions, we compared genome-wide DNA methylation patterns in seedlings of wild-type plants and an Arabidopsis line lacking all three H1s. In plants, cytosines are methylated in three different sequence contexts: CG, CHG and CHH, (H denotes adenine, cytosine or thymine). The global distribution of DNA methylation on transposons in the triple *h1.1h1.2h1.3* mutant was found to be similar to that reported for a double *h1.1h1.2* mutant (Zemach et al., 2013) (Supplemental Fig. S19; Supplemental Tables S5, S6), consistent with the limited global role of H1.3 in affecting DNA methylation under normal (non-H1.3-inducing) growth conditions. We then examined whether the regime of combined low light/drought used in this study and referred to as 'stress conditions' under which H1.3 is strongly induced, produced alterations in DNA methylation, and if any of the observed changes were dependent on H1.3. To this end, we compared the effect of stress on the global level of DNA methylation in the CG, CHG and CHH contexts, in wild-type plants and the *h1.3* mutant, by BS-seq. Overall, stress treatment resulted in increased total DNA methylation, which is consistent with the recent finding that hypermethylation is the prevalent mode of differential methylation in Arabidopsis grown at low water potential (Colaneri and Jones, 2013). Our analysis established the average level of DNA methylation at hundreds of locations. The fluctuations in such averages are naturally quantitatively low, but measurable, reproducible between replicates and statistically significant. We found that the relative increase was moderate in the CG context (2.5%), higher in the CHG context (9.3%) and particularly pronounced in the CHH context (31.8%) (Fig. 8A).

As expected, in *h1.3* mutant plants in control conditions, the absence of H1.3 affected the global DNA methylation level only slightly, as revealed by the small overall hypomethylation in the CHG context. However, the lack of H1.3 significantly diminished stress-related DNA methylation, with the most pronounced relative decrease in the CHH context (Fig. 8A; Supplemental Table S7).

From our whole-genome methylome data we identified genic and non-genic sequences with methylation signatures in all three contexts that increased most significantly in wild-type plants in response to stress. Closer inspection of these stress-responsive loci showed that in control conditions their basal methylation level in *h1.3* plants was slightly higher than in the wild-type. However, upon stress these loci did not respond in the *h1.3* mutant as dramatically as

401 in the wild-type. This applied to all contexts, suggesting that H1.3 may be required for the
402 occurrence of this increased methylation (Fig. 8B, Supplemental Fig. S20).

403 We next examined which chromatin regions are differentially methylated upon stress in the
404 wild-type and *h1.3* mutant lines. In Arabidopsis, transposons comprise at least 10% of the
405 genome, i.e. one-fifth of the intergenic DNA (Arabidopsis Genome, 2000). The analysis of two
406 sets of transposons, one with high (heterochromatic TEs) and the other with low (euchromatic
407 TEs) levels of H3K9me2, showed that upon exposure to stress, changes in DNA methylation in
408 both wild-type and *h1.3* mutant lines affected the former TEs to a much greater extent than the
409 latter (Supplemental Fig. S21).

410 In wild-type plants, among 5030 differentially methylated regions (DMRs) most strongly
411 affected in the CHH context in response to stress, 2908 were TEs and 371 were genes
412 (sometimes a single DMR contained both a TE and a gene). In the *h1.3* mutant, in the same CHH
413 context, the 3742 DMRs included 2217 TEs and 270 genes. For both wild-type and *h1.3* plants,
414 GO analysis of genes present in DMRs did not reveal any specific functional classes, in
415 particular those related to stress response. However, an examination of the specific types of TEs
416 enriched in DMRs in the CHH context, revealed that in response to stress, there were relatively
417 fewer transposons of the RC/Helitron family in the *h1.3* line compared to the wild-type, while
418 the opposite was true for transposons of the LTR/Gypsy family.

419 While the proportion of TEs/genes in stress-related DMRs appeared similar in wild-type
420 and *h1.3* mutants (about 8:1), the overlap of methylated sequences between these two lines is
421 only 25%. Thus, the loss of H1.3 significantly affected not only the amount, but also the
422 sequence specificity of stress-related CHH methylation.
423

Discussion

Localization and *in vivo* properties of H1 variants as revealed using H1-GFP-fusion proteins

Rather than studying H1 transcript abundance, we analyzed transgenic Arabidopsis lines expressing fusions of GFP with each of the three H1 variants under the control of their native promoters. This showed that the stress-inducible H1.3 protein occurs in Arabidopsis as two apparently independent pools, which we defined as the constitutive- and facultative pools. The former is restricted to guard cells, in which H1.3 occurs under both normal and stress conditions, while the latter includes H1.3 that appears only upon induction and is localized in various tissues and organs. This is in stark contrast to the main variants, H1.1 and H1.2, which are stably expressed throughout the plant. The occurrence of a constitutive guard cell-specific H1.3 pool is consistent with earlier microarray expression data showing that under normal growth conditions the *H1.3* transcript is the second most abundant of 64 transcripts preferentially expressed in Arabidopsis guard cells but not in mesenchymal cells (Leonhardt et al., 2004). We found that as in water-stress conditions, ABA is a major positive determinant of the facultative pool of H1.3 induced by low light stress. Thus, might ABA also be responsible for maintaining the constitutive pool of this protein in guard cells? While this still requires experimental confirmation, we consider such a possibility highly plausible in the light of a recent report that guard cells are capable of autonomous ABA synthesis (Bauer et al., 2013). Moreover, the earlier finding that the level of *H1.3* transcript in guard cells did not change upon ABA treatment (Leonhardt et al., 2004), suggests that it is already at saturation level, and that the constitutive H1.3 pool in guard cells may not be significantly affected by stress.

Our FRAP analyses of the *in vivo* behavior of H1 variants in nuclei revealed that H1.3 binds chromatin with significantly faster dynamics than the more slowly exchanging main variants, particularly the dominant variant H1.2, and in contrast to the main variants, it shows no stable bound pool. To better understand the possible underlying causes of the differences in chromatin binding between the main and stress-inducible linker histone variants, we compared (i) their overall protein organization (Supplemental Fig. S22A) and (ii) 3D molecular models of their conserved globular domains (GH1s) (Supplemental Fig. S22B,C). The C-terminal domain (CTD) of H1.3 is about 50% shorter and has a reduced overall positive charge, compared with

those of H1.1/2 (Supplemental Fig. S11). Both the N- and C-terminal domains of Arabidopsis H1.3 lack the (S/T)PXK motifs that enhance DNA-binding and are present in the corresponding domains of H1.1 and H1.2 (Supplemental Fig. S22A). The GH1s of the H1.1/2- and H1.3-type differ by a minor alteration of three amino acids that provides the basis for phylogenetic separation of the two protein clades. The amino acids E66, R112 and S116 in H1.1/2-type histones become F28, N75 and K79 in H1.3-type histones. Interestingly, these three amino acids are located close to each other on the surface of GH1 (Supplemental Fig. S22C). In addition, R112 in *A. thaliana* H1.1/2 corresponds to R74 in the human H10 histone variant, identified as a binding Site 1 residue by Brown and colleagues (Brown et al., 2006). The remaining two amino acids, E66/F28 and S116/K79, are located between residues corresponding to DNA binding Site 1 (H62, R103, K104, K111, R112, K121, K123 in H1.1/2; H24, R66, K67, K74, K84, K86 in H1.3) and Site 2 (R79, K127, K118 in H1.1/2; K41, K90, K81 in H1.3). We conclude that these amino acid replacements, together with the shortened CTD, could influence the binding of H1.3 and explain its increased mobility. Another recent study utilizing FRAP showed that H1-chromatin binding is dynamic, with a significant fraction of H1 molecules being partially bound in metastable states that can be readily competed against (Stasevich et al., 2010). Indeed, in addition to its molecular structure and post-translational modifications, one of the key factors affecting the interaction of H1 with chromatin, is competition for specific chromatin binding sites. The incremental increase in the concentration of competitors, like other H1 variants or HMG proteins, was shown to lead to a new steady state with a shorter H1 chromatin residence time (Catez et al., 2004, Catez et al., 2006). H1.3, which in most tissues increases incrementally upon stress, shows exceptionally high mobility and lacks any stable bound fraction, is ideally suited to act as a general competitor with the main H1 variants throughout the entire chromatin fiber. Interestingly, under stress conditions we observed shortening of the residence time of the dominant H1.2 variant in non-guard cell tissues, which approached the value of its typical residence time in guard cells. This raises the question of whether the potential effect of H1.3 as a competitor is spread evenly among all H1 binding sites, or shows some degree of specificity. To address this issue, we mapped the distribution of all three H1 variants along Arabidopsis chromosomes. The measurement of genome-wide histone occupancy preferences by ChIP-chip was not expected to yield localized enrichment comparable to that seen for specifically targeted binding proteins such as RNA polymerase. However, we did observe clear and statistically

significant differences between the profiles of the H1 variants on large groups of genes and other sequences. As expected for linker histones, both the main and stress-inducible variants were highly enriched in heterochromatin, but they also occurred in genic regions. Notably, the proportions of relative enrichment between the stress-inducible and main variants changed in favor of the former in genic compared to typical heterochromatin regions. Interestingly, we observed differences in the distribution of intensity profiles along chromosomes between the main- and stress-inducible variants, which were consistent with patterns of staining with H1 variant-specific antibodies (Ascenzi and Gantt, 1999b) and imply some underlying differences in chromatin localization preferences. To elucidate the possible reasons for these differences, we analyzed correlations between the distribution of H1 variants and the known distribution profiles of H3K4me3 and H3K9me2 methylation marks, the two functionally opposed epigenetic signatures associated with transcriptionally active and repressive chromatin states, respectively. Besides the generally similar tendency of all three H1 variants to accumulate in H3K9me2-rich heterochromatin, H1.3 showed by far the weakest negative correlation with the functionally opposite H3K4me3 epigenetic mark (Fig. 7A). Moreover, and in contrast to H1.1 and H1.2, among genes known to be enriched in H3K4me3, H1.3 showed a marked preference for those with the highest level of this mark. This suggests that upon induction, H1.3 may compete particularly strongly with the main variants in heterochromatin regions in which the H3K4me3 signatures of past or present transcription have been retained. A more in-depth analysis is required to explain the increased preference of H1.3, in relation to the main variants, for H3K4me3 marked chromatin. This could involve examination of the binding properties of Arabidopsis H1 variants to *in vitro* reconstituted nucleosomes.

In summary, our data reveal two likely separate and autonomous pools of H1.3 in Arabidopsis: a constitutive guard cell pool and an environmentally-regulated facultative pool in other tissues. The super-fast binding dynamics and lack of a stable bound fraction of H1.3 shown by FRAP analysis, confer significant advantages for a potential competitor targeting H1-binding sites in chromatin. In addition, our mapping of global H1.3 occupancy in chromatin reveals that while binding mostly within heterochromatin, this linker histone shows a measurable preference, in comparison with the main variants, for chromatin with epigenetic signatures of active transcription. These findings raise the interesting question of whether the role of the inducible pool of H1.3 in non-guard cell tissues is the same or different from that it plays in guard cells.

The ratio of non-synonymous substitutions per non-synonymous site to synonymous substitutions per synonymous site (Ka/Ks) for the main and stress-inducible H1 variants of Arabidopsis is 0.29, which is consistent with strong purifying selection acting on proteins of the two clades and suggests that this diversification plays an adaptive role. Interestingly, we found an early separation of the main and stress-inducible variants, broadly coincidental with an ancient gene or even genome duplication in the common ancestor of extant angiosperms (Jiao et al., 2011). *Amborella trichopoda*, a member of the Amborellales, the earliest angiosperm branch (Magnoliophyta), has both H1.1/2-like and H1.3-like variants with their characteristic globular domains and differences in the length of their C-terminal domains. However, the GH1s from mosses, ferns or gymnosperms cannot be precisely classified into main and stress-inducible variants (Supplemental Figs. S12- S14).

Consequences of depletion of the H1.3 variant under normal and stress conditions

The availability of *h1.3* null mutant lines enabled assessment of the role of H1.3 in plants grown in normal and stress conditions. We found that wild-type and *h1.3* plants grown under non-stress conditions were of similar size, but the mutant plants showed a reduced CO_2 assimilation rate and their young leaves had a decreased stomatal density. Comparison of the transcriptomes of wild-type and *h1.3* plants grown under non-stress conditions showed that among genes with altered transcription in the mutant, there was a significant enrichment of those known to be expressed specifically in guard cells or in guard cells and other tissues, many of which have been linked with guard cell functions. Given the constitutive occurrence of H1.3 in guard cells, this finding suggests that it could be involved in controlling at least some genes specifically expressed in these cells and is probably required for their normal physiological functions. Strikingly, the genes mis-regulated in the *h1.3* mutant also included major regulators of stomatal biogenesis, known to be expressed in stomatal progenitor cells rather than in mature guard cells. While the direct involvement of H1.3 in the regulation of these genes cannot be excluded, it is also possible that the observed effect is indirect and results from some negative influence on stomatal development in younger leaves, exerted by physiologically impaired guard cells in mature leaves (Lake et al., 2001).

To increase the chances of identifying differences in the responses of wild-type and *h1.3* mutant plants to environmental perturbations, we subjected these plants to combined low light

548 and water stress, as both treatments cause the induction of H1.3. Surprisingly, we found that a
549 combination of the two stresses led to a synergistic rather than an additive increase in the level of
550 H1.3 induction. Moreover, there were notable differences between wild-type and *h1.3* plants in
551 their responses to combined stress. The typical adaptive developmental response of Arabidopsis
552 to mild water deficiency, i.e. growth retardation resulting mainly from decreased accumulation
553 of biomass after stomatal closure, was visibly hampered in *h1.3* plants, which had a higher leaf
554 number and larger dry and fresh mass compared to wild-type plants. Acceleration of generative
555 development, another adaptation to stress, was also hampered in *h1.3* plants. Overall, the *h1.3*
556 plants reacted as if they were unable to mount a typical adaptive response to drought stress. With
557 regard to biomass accumulation, the maximum capacity of leaves for exchanging CO_2 and water
558 is mainly determined by short-term regulation of stomatal aperture and long-term regulation of
559 their density through the control of stomatal development (Doheny-Adams et al., 2012).
560 Compared to the wild-type, *h1.3* plants showed a decreased ability to respond to combined stress
561 by down-regulating stomatal density, which may indicate their impaired potential for adjusting
562 stomatal development to a changing environment. Again, as indicated above with respect to the
563 decreased stomatal density in *h1.3* plants in non-stress conditions, the role of H1.3 in this
564 regulation may be either direct or indirect, and has yet to be determined. In the short term, the
565 regulation of stomatal function might have been directly affected by the aberrant activity of some
566 guard cell-specific genes mis-regulated in H1.3-depleted plants. However, the impairment of
567 stomatal function and probably stomatal development as well, may not be the only causes of the
568 observed lack of adaptive developmental plasticity in response to low light/drought stress. Our
569 analysis showed that the transcriptional response of *h1.3* mutants to combined stress differed
570 considerably from that of wild-type plants and revealed that in the absence of H1.3, 70% of over
571 1700 affected transcripts were down-regulated. Therefore, it is possible that the growth habit of
572 *h1.3* plants under stress could also be partly due to defects in non-stomatal stress response
573 pathways. Importantly, the normal stress response of *h1.3* mutant plants complemented with the
574 *H1.3* gene confirmed that the lack of H1.3 was the major cause of all aspects of the observed
575 phenotypes.

576 We found that Arabidopsis plants subjected to combined low light/drought stress
577 responded by increased DNA methylation, particularly in the CHH context. The recent
578 demonstration of the key role of Arabidopsis H1.1 and H1.2 in preventing the access of DNA

579 methyltransferases to chromatin DNA (Zemach et al., 2013), prompted us to examine the role of
580 H1.3 in stress-related changes in DNA methylation. In control conditions, the triple *h1.1h1.2h1.3*
581 mutants showed changes in the global DNA methylation profile that were very similar to those
582 seen in the double *h1.1h1.2* mutant (Zemach et al., 2013). This indicates that H1.3 plays only a
583 minor role in maintaining the pattern of DNA methylation under normal growth conditions.
584 However, the depletion of H1.3 significantly decreased stress-related DNA hypermethylation
585 and affected its sequence localization. This suggests that the stress-induced H1.3 variant may
586 interfere with the suppression of DNA accessibility to methyltransferases caused by H1.1 and
587 H1.2.
588
589
590 ## Conclusions
591 The properties of the stress-inducible H1.3 variant described in this report are consistent
592 with a function as a general factor capable of facilitating chromatin accessibility, most likely by
593 directly competing for binding sites with the main H1 variants. The strong dependence of the
594 environmentally controlled facultative pool of H1.3 on ABA and decreased light intensity as well
595 as its relative insensitivity to major photoreceptors, suggest a major role for retrograde
596 chloroplast-to-nucleus communication in *H1.3* induction. This is consistent with earlier reports
597 that *H1.3* is one of a small number of genes comprising a core response module responsible for
598 plastid-to-nucleus signaling (Glasser et al., 2014) and regulation of redox homeostasis
599 (Khandelwal et al., 2008). The existence of an autonomous and constitutive guard cell-specific
600 pool of H1.3, as well as the importance of H1.3 in maintaining leaf stomatal density, suggest that
601 chromatin in guard cells may require permanent modulation by this linker histone variant for
602 proper functioning. Further studies are required to uncover the underlying molecular causes and
603 biological significance of the revealed subtle preference of H1.3 for epigenetic signatures of
604 transcriptionally active chromatin, and to elucidate the possible role of H1.3 in stomatal
605 development. The fact that stress-inducible linker histones of the H1.3-type subfamily are
606 conserved in Angiosperms, but appear to be absent in evolutionarily older plant lineages,
607 indicates that their biological function may have been important in the evolution of the currently
608 most abundant group of plants on Earth.
609

Materials and Methods

Plant material

We used *Arabidopsis thaliana* lines in the Columbia (Col-0) ecotype background unless stated otherwise. Mutants *h1.1* (SALK_N628430, (Rea et al., 2012)) and *h1.2* (GK-116E080) were obtained from the European Arabidopsis Stock Center. *h1.3* in the Landsberg *erecta* (L*er*) background was obtained from the Cold Spring Harbor Laboratory collection (GT18298). The *h1.1h1.2h1.3* triple mutant was obtained by crossing double mutant *h1.1h1.2* with *h1.3* (which had previously been backcrossed four times to the Col-0 background). Primers used for genotyping *h1* mutants are listed in Table S7. Double mutants *phyAphyB* and *cry1cry2* were provided by Stanislaw Karpiński (Banas et al., 2011). *aba1* (Ler) was provided by Tomasz Sarnowski and Csaba Koncz (Strizhov et al., 1997). Transgenic line H2B-YFP was provided by Klaus Grasser (Launholt et al., 2006). Transgenic lines encoding linker histone variants H1.1 and H1.2 tagged with EGFP, promH1.1::H1.1-EGFP and promH1.2::H1.2-EGFP, were described previously (She et al., 2013). The line expressing H1.3 tagged with EGFP was obtained analogously: a genomic fragment containing the promoter, coding region except for the stop codon and terminator was amplified by PCR using specific primers listed in Table S7. The obtained cassette was cloned into vector pCambia0390 carrying the *nos:bar* gene. This construct was then introduced into *Agrobacterium tumefaciens* (GV3101). To obtain the prom.H1.3::H1.3-EGFP and *h1.3*/prom.H1.3::H1.3-EGFP lines, wild-type Arabidopsis plants (Col-0 and Ler) and *h1.3* (Ler) were respectively transformed using the floral dip method (Clough and Bent, 1998). Transformed seeds were selected on soil sprayed with Basta solution (50 µg/ml). At least 12 lines with a confirmed GFP signal were obtained for each construct. After segregation analysis, single insertion and homozygous lines from the T3 or T4 generations were identified and used for further experiments (2 lines for H1.3-GFP and 3 lines each for H1.1-GFP and H1.2-GFP). Expression of EGFP-tagged H1s was confirmed using a fluorescence microscope.

Plant growth and treatment conditions

For all analyses, except the experiments with combined low light and drought treatments, plants were grown on plates in medium containing ½ Murashige and Skoog (MS) salts (Sigma-Aldrich) and 1% (w/v) agar, pH 5.8, or in soil under long-day conditions (16 h light/8 h dark) at 22°C,

with 70% relative humidity (RH) and illumination of 120 µmol m^{-2} sec^{-1}. For analysis of the effects of limited light (low light conditions), the intensity of light during the day was reduced to ~20 µmol m^{-2} sec^{-1} when seedlings were 21-days old, and the plants were kept in these conditions for 4 days. To investigate morphological and physiological responses to combined low light and drought, plants were sown in ø 27-30 Jiffy expandable peat pots. At the third-leaf stage (16 days after sowing) six peat pots were buried in a single large plastic pot (4.5 dm^3) filled with a strong loamy sand:sand mixture (7:2 v:v). In each large pot, plants of *h1.3*, its sibling wild-type (WT) and *h1.3* complemented with prom. H1.3::H1.3-EGFP (*h1.3*/H1.3-GFP) were placed in equal number. At this stage, only one plant of equal size was left in each single peat pot. Immediately, or after two weeks of growth [25°C, PFD 250 µmol m^{-2} s^{-1} provided by HPS lamps 'Agro' (Philips, Brussels, Belgium), photoperiod 14/10, RH = 40%], the plants were divided for four experimental series (light source, photoperiod and RH as before): control (400 µmol m^{-2} s^{-1}) or low light (40 µmol m^{-2} s^{-1}), combined with one of two watering regimes, i.e. control – 60% field water capacity (FWC) regulated by daily water supplementation to maintain an equal mass, or drought – field water content in soil gradually reduced to 20% FWC (water controlled daily, as for the control). The treatments were applied for 17 days, after which growth/physiological analyses were performed.

Measurements of physiological and morphological parameters

Each parameter was measured for at least 8 replicate plants for the wild-type (WT), *h1.3* mutant *(h1.3)* and complemented *h1.3* mutant (*h1.3*/H1.3) grown under control, low light, drought and low light/drought conditions.

Net photosynthetic rate (Pn) was measured using an infrared gas analyzer (Ciras-1, PP Systems, Hitchin, Herts., UK), with a whole plant chamber (200 cm^3). The irradiation system was equipped with halogen lamps. The flow rate of air with a constant CO_2 concentration [400 µmol(CO_2) mol^{-1}(air)] through the assimilation chamber was 600 cm^3 min^{-1}. Measurements were performed at 25°C (leaf temperature), at PFD 500 µmol(quanta) m^{-2} s^{-1} and RH of 50%. The 'A' value was then calculated (Parkinson et al., 1980).

Water relations in leaves were characterized by determining the relative water content (RWC) and water content (WC). Measurements were performed using all leaves detached from the plants. RWC was determined using the equation RWC = (FW - DW) x $(TW - DW)^{-1}$ x 100%

672 (Klepper and Barrs, 1968); where FW is fresh weight, DW is dry weight and TW is turgid
673 weight. To measure TW, leaves were placed in darkness for 24 hours in vials containing water,
674 at 5°C, to permit complete rehydration. Plant material was dried at 70°C. WC was calculated as
675 $WC = (FW - DW) \times DW^{-1} \times 100\%$.
676 ***Analysis of plant growth*** included recording of the following parameters: leaf number, stem
677 length, leaf area, and fresh and dry weight of leaves and stems. Leaf area was measured using a
678 scanner (ScanMaker 3880, Microtek, Hsinchu, Taiwan) and Delta-T Skan 2.03 software (Delta-T
679 Devices, Cambridge, UK).
680 ***Leaf chlorophyll content*** was measured with a SPAD-502 chlorophyll meter (Konica Minolta,
681 Tokyo, Japan). SPAD readings were taken from all leaves larger than the measurement window
682 (2 x 3 mm).
683 ***Chlorophyll 'a' fluorescence.*** Chl fluorescence images of whole plants were taken using an
684 imaging fluorometer (FluorCam, PSI, Brno, Czech Republic) (Nedbal L., 2004). Chlorophyll
685 fluorescence induction kinetics and quenching parameters were evaluated at 20°C and a normal
686 CO_2 molar ratio, with an experimental protocol comprising 20 min of dark adaptation, and the
687 following measurements: (a) Fo – fluorescence of dark-adapted leaves when all PSII reaction
688 centers are open; (b) Fm – fluorescence of dark-adapted leaves when all PSII reaction centers are
689 closed after a light saturating pulse of about 2000 μmol m^{-2} s^{-1}; (c) Fs – steady-state fluorescence
690 in light-exposed leaves after 420 s of actinic light (300 μmol m^{-2} s^{-1}) combined with saturating
691 light pulses given every 25 s; (d) Fm' – fluorescence of light-adapted leaves when all PSII
692 reaction centers are closed during the last saturating pulse; and (e) Fo' – fluorescence of light-
693 adapted leaves when all PSII reaction centers are open, measured with the actinic light source
694 switched off after the far-red light pulse. The photochemical quenching coefficient (qP)
695 (Klughammer and Schreiber, 1994) and non-photochemical quenching (NPQ) (Bilger and
696 Bjorkman, 1991) were then calculated. The actual or effective quantum yield of photochemical
697 energy conversion in PSII (ΦPSII) (in the light-adapted state) was then defined (Genty et al.,
698 1989).
699 ***Determination of ABA content.*** ABA was measured by ELISA as described previously (Dubas
700 et al., 2013). For each treatment, at least three independent ABA measurements were performed
701 on pooled samples collected from three different plants.
702

Sequence identification and multiple sequence alignment

Arabidopsis proteins possessing a GH1 domain were identified by exhaustive PSI-BLAST searches of the *A. thaliana* proteome, using the GH1 domain of Arabidopsis histone H1.1 as the query sequence. For each identified *A. thaliana* protein, a PSI-BLAST (Altschul et al., 1997) profile (3 iterations, threshold 0.001) was built for its GH1 domain using the NCBI non-redundant (nr) sequence database, and mapped against the TAIR database. Plant sequences possessing the GH1 domain were obtained from the NCBI nr database by transitive PSI-BLAST searches (3 iterations, threshold 0.001) using all *A. thaliana* GH1 proteins as queries. The sequences were classified into SMH, HMG and H1 groups based on sequence similarity in a graphical clustering tool (CLANS) (Frickey and Lupas, 2004). Multiple sequence alignment of the GH1 domain was performed using PCMA (Pei et al., 2003) and Mafft (Katoh and Standley, 2013) followed by some manual adjustments. Sequence conservation in the GH1 domain for H1.1/2-like and H1.3-like variants was visualized from the respective multiple sequence alignments using WebLogo (Crooks et al., 2004).

Model building

To identify an optimal template for GH1 domain model building, the sequences of all *A. thaliana* H1 histone variants were submitted to Meta-Server, which is an assembly of various secondary structure prediction and state-of-the-art fold recognition methods. Collected predictions were screened with 3D-Jury (Ginalski et al., 2003), the consensus method of fold recognition servers, and the structure of *G. gallus* GH5 protein (pdb|1hst) (Ramakrishnan et al., 1993) was chosen as the template. A sequence-to-structure alignment between H1.1, H1.2, H1.3 histone variants and the template was built manually using the 3D assessment procedure (Ginalski and Rychlewski, 2003), taking into account the predicted secondary structure, hydrophobic profile of the family and conservation of important residues. Based on the final sequence-to-structure alignment, 3D models of all three *A. thaliana* histone H1 variants were built with the MODELLER program (Sali and Blundell, 1993). Finally, side-chain rotamers in the models were optimized using the SCWRL4 package (Krivov et al., 2009).

Domain architecture and sequence analysis

To detect other conserved domains in all identified *A. thaliana* GH1 domain proteins, their sequences were analyzed with CDD (Marchler-Bauer et al., 2011) and SMART (Letunic et al., 2006). This analysis also included searches for transmembrane segments (with TMHMM2), signal peptides (SignalP) (Nielsen et al., 1997), low compositional complexity (CEG) (Wootton, 1994) and coiled coil regions (Coils2) (Lupas et al., 1991), as well as internal repeats (Prospero) (Mott, 2000). Regions with no significant sequence similarity to known protein domains were submitted to Meta-BASIC (Ginalski et al., 2004) and then to Meta Server coupled with 3D-Jury. All identified domains were checked for the conservation of essential elements, including the presence of domain-specific residues.

The percentages of positively (R, K) and negatively (D, E) charged residues as well as selected hydrophobic amino acids (V, L, I) in *A. thaliana* H1 histone variants were established separately for the GH1 domain and N- and C-terminal unstructured regions. The sequences were also searched for the presence of (S/T)PXK DNA binding motifs. In addition, the charge profile in the C-terminal domain was established by calculating the net charge in a 10 amino-acid sliding window.

Tree building

Phylogenetic trees for selected H1 histone variants from *A. thaliana* as well as a broader tree for plant histone H1 proteins, were calculated with maximum likelihood (PhyML) (Guindon et al., 2010). The multiple sequence alignment of the GH1 domain used for phylogeny reconstruction was additionally trimmed to eliminate poorly aligned and thus uninformative regions (TrimAl) (Capella-Gutierrez et al., 2009). Branch support values were calculated using the aLTR method (Anisimova and Gascuel, 2006). Trees were drawn with iTOL (Letunic and Bork, 2011). A coding sequence alignment for Ks/Ka ratio estimation was prepared with ParaAT (Zhang et al., 2012b). The Ks/Ka ratio was calculated in KaKs_Calculator using all of the implemented methods (Zhang et al., 2006) and this ratio was averaged over all the predictions. Plant H1 protein sequences were also clustered in the 3D mode in CLANS (Frickey and Lupas, 2004) with a p-value threshold of 1e-06.

Gene expression analysis (RT-qPCR)

763 Total RNA was isolated using TRI-Reagent (Sigma Aldrich), followed by Turbo DNase
764 treatment (Ambion). The quantity and quality of RNA were measured with a NanoDrop ND1000
765 spectrophotometer (Nanodrop technologies), by gel electrophoresis and/or Bioanalyzer 2100
766 (Agilent Technologies). Reverse transcription (RT) was performed using random hexamer
767 primers with a Transcriptor First-Strand cDNA Synthesis Kit (Roche). The obtained cDNA was
768 diluted and used as the template in qPCR with LightCycler 480 SYBR Green I Master mix
769 (Roche). Primers used for the amplification of specific cDNAs for expression analysis are listed
770 in Table S7. Reactions were run on a Roche Light Cycler 480.
771
772 Microarray gene expression experiments
773 Material was collected from 24-day-old WT and *h1.3* seedlings grown under control and 4-day
774 low light conditions in the first experiment, and from the leaves of 5-week-old WT and *h1.3*
775 plants grown under control and combined low light and drought conditions in the second
776 experiment. Total RNA was extracted using TRI-Reagent (Sigma-Aldrich), followed by
777 treatment with Turbo DNase (Ambion) and a RiboMinus™ Plant Kit (Invitrogen) to reduce the
778 rRNA fraction. The quantity and quality of the isolated RNA was determined using a NanoDrop
779 ND1000 spectrophotometer and RNA integrity was assessed with a Bioanalyzer 2100 100 ng of
780 RNA were used for cDNA synthesis with an Ambion WT Expression Kit. 5.5 µg of cDNA, after
781 fragmentation and labeling with a GeneChip WT Terminal Labeling Kit (Affymetrix), were
782 hybridized with an Agronomics array (Rehrauer et al., 2010) using a GeneChip Hybridization
783 Wash and Stain Kit, according to the manufacturer's recommendations (Affymetrix). Three
784 biological replicates were examined for each genotype.
785 Probe intensities for strand-specific signals were extracted using Affymetrix apt-cel software.
786 The signal was normalized separately for each of the three biological replicates and the average
787 of the replicates for each probe was used. Probe positions were transformed to the TAIR10
788 genome assembly and the average probe signal for all genes, annotated in the TAIR10 genome
789 release, was calculated. Differential gene expression was computed by taking the logarithm of
790 the fold change between the relevant conditions. Up- and down-regulated genes were defined as
791 those with absolute z-scores for log-fold changes of >2.0. Submission of the microarray data to
792 the ArrayExpress submissions system is in progress.
793

794 Fluorescence and confocal microscopy

795 GFP fluorescence was visualized using a Nikon C1 Laser Scanning Confocal System.

796

797 FRAP analysis

798 Fluorescence Recovery After Photobleaching (FRAP) analysis was performed using a Leica
799 TCS-SP2 confocal laser scanning microscope. Analyses were performed for leaves, roots, root
800 meristems and hypocotyls derived from 21-day-old seedlings of the following lines grown under
801 control and 4-day low light conditions: promH1.1::H1.1::GFP, promH1.2::H1.2::GFP,
802 promH1.3::H1.3::GFP and prom35S::H2B::YFP.
803 Fluorescence intensity was measured for each studied plant after photobleaching. Measurements
804 were taken at 0.6, 0.8, 1.0, 1.2 and 5.0 s, and then at 5 s intervals until 70 s after photobleaching,
805 resulting in 18 measurements per nucleus. Several nuclei were examined in this way for each
806 genotype. The raw data were normalized to the 100% value just before the moment of bleaching.
807 The measurements for each genotype were then averaged, resulting in a single curve per
808 genotype, to which the model was fitted. The GFP fluorescence intensity after photobleaching
809 was modeled using the parametric exponential model (Launholt et al., 2006):

810 (*) $$frap(t) = \alpha\left(1 - e^{-t/\tau}\right) + \beta;$$

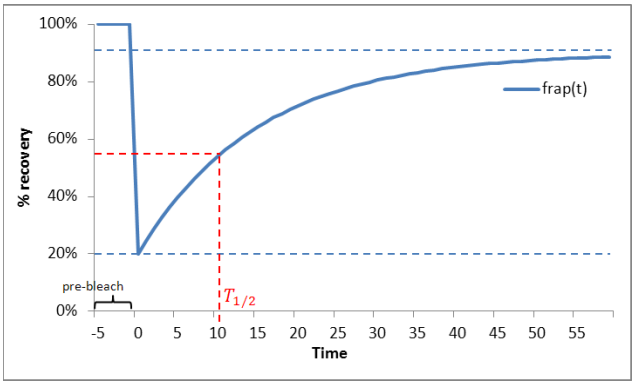

811

812

813 The time to half-recovery of the fluorescence intensity, derived directly from the model equation,
814 is marked below as $T_{1/2}$:

815 $$\alpha\left(1 - e^{-T_{1/2}/\tau}\right) + \beta = \left\{\lim_{t\to\infty}\left[\alpha\left(1 - e^{-t/\tau}\right) + \beta\right] = \alpha + \beta\right\} = \frac{1}{2}\alpha + \beta$$

$$T_{1/2} = \tau \ln(2)$$

Estimation of model parameters. Model parameters were obtained using the Newton-Raphson optimization algorithm that minimized the sum of squared deviations between the fitted curve and the measurements. To ensure the optimal starting point for the algorithm, an initial search of three-dimensional parameter space (α, β, $T_{1/2}$) was performed. Parameters α and β were tested in the interval (0, 1) at intervals of 0.1, and the $T_{1/2}$ in the interval (0, 100) at intervals of 1. The first one thousand combinations that resulted in the lowest objective function value were used as starting points for the optimization algorithm. The solution that provided the best curve fit to the empirical data indicated the vector of model parameters. For unconstrained estimates, the covariance matrix of model parameters is defined by the following formula:

$$\boldsymbol{\Sigma} = MSE * (\mathbf{H})^{-1}$$

$$MSE = \mathbf{r}^T \mathbf{r} \Big/ (n - p)$$

$$\mathbf{r} = \left(frap(t) - \hat{frap}(t) \right)$$

where $\boldsymbol{\Sigma}$ is the (3x3) parameter's covariance matrix, **H** is a numerical approximation of the Hessian matrix (3x3) of the objective function, n is the number of observations (18), p is the number of estimable parameters (3), and $\left(frap\,(t) - \hat{frap}(t) \right)$ represents the difference between the observed measurement and the fitted value. The optimization was performed with SAS 9.2 software using the **IML** procedure (SAS Institute Inc., 2010), and **call nlpnra** was used as the optimization algorithm. The mobile fraction (Mf) for each of the histone variants was calculated (Launholt et al., 2006). Each parameter is provided with the standard error of this estimate (these are not 95% confidence intervals). The standard errors of the model parameters and estimates of the mobile fraction were obtained from the covariance matrix $\boldsymbol{\Sigma}$.

ChIP-chip experiments.

ChIP experiments were performed as described previously (Nelson et al., 2006), with some modifications. 24-day-old seedlings of wild-type (Col-0), promH1.1::H1.1::GFP, promH1.2::H1.2::GFP and promH1.3::H1.3::GFP lines, grown under control and 4-day low light conditions were used as the source of chromatin. Anti-H3 (ab1791, abcam) antibody bound to Dynabeads Protein A (Invitrogen) or GFP-Trap-A (Chromotek) were incubated with isolated chromatin. The extracted DNA was resuspended in 100 µl of water. ChIP enrichment for linker histones and H3 targets was determined by qPCR using LightCycler 480 SYBR Green I Master

mix (Roche). Reactions were performed with 2 µl of immunoprecipitated DNA as template. A standard curve was established for each pair of primers. The amount of ChIP DNA was calculated based on the standard curve and input DNA was used as a control. For ChIP-chip experiments, the extracted DNA was amplified using a WGA2 Kit (Sigma-Aldrich) according to the manufacturer's protocol. 1.5 µg of DNA were used for fragmentation and labeling with a GeneChip WT Terminal Labeling Kit (Affymetrix). Labeled DNA was hybridized to the Agronomics microarray (Rehrauer et al., 2010) using a GeneChip Hybridization Wash and Stain Kit according to the manufacturer's recommendations (Affymetrix).

Microarray probe signals were extracted using Affymetrix apt-cel software. Signals for both strands were merged and the replicates were then transformed to TAIR10 coordinates, normalized and averaged in the same way as the RNA expression data. Ln(IP/Input) was computed for every probe and the significant regions were then called by finding regions of length >15 probes with enrichment >0.5 (excluding at most 3 faulty probes). Occupancy profiles were computed as average signals for 100-bp windows, beginning at the 5' and 3' ends of respective features, such as the 5' and 3' ends of genes. All expression plots were drawn using the agronomics python package available from http://bioputer.mimuw.edu.pl/software/agronomics

BS-seq

For global DNA methylation analysis, DNA was extracted from leaves of 5-week-old wild-type (WT) and *h1.3* plants grown under control and low light/drought conditions. Bisulfite sequencing (BS-seq) was performed in the GeneCore Facility Center, EMBL using an Illumina HiSeq2000, with a 100-bp read length.

Reads from BS-seq were mapped to the TAIR10 genome assembly using Bismark software (Krueger and Andrews, 2011). The positions of methylation sites were extracted with Bismark-extractor and filtered to exclude those without coverage of at least 10 reads. The positions were then divided into groups containing cytosines in three different contexts (CG, CHG and CHH) and the methylation ratios were computed both for each cytosine separately as well as in 50- and 100-bp windows along all chromosomes. The averaged methylation level in each context (CG, CHG and CHH) throughout the whole genome was calculated for the 100-bp bins.

Accession numbers

Data from high-throughput sequencing experiments are being submitted to the ArrayExpress submissions system data collection under the following accession numbers: E-MTAB-2804 for analysis of genomic distribution of three linker histone variants in Arabidopsis under normal and low light conditions by ChIP-chip; E-MTAB-2806 for transcriptomic profiling of the response to combined low light and drought conditions in wild type and h1.3 mutant plants; E-MTAB-2807 for bisulfite sequencing of the wild type and linker histone mutants under control and combined low light and drought conditions. They are also available at http://bioputer.mimuw.edu.pl/data/H1.

Acknowledgments

We thank Gideon Grafi, Célia Baroux and John Gittins for critically reading the manuscript. We also thank Klaus D. Grasser for the H2B-YFP transgenic line, Stanisław Karpiński for providing *phyAphyB* and *cry1cry2* mutants, and Tomasz Sarnowski and Csaba Koncz for providing the *aba1* mutant. Furthermore, we thank Vladimir Benes and Dinko Pavlinic from the EMBL GeneCore sequencing team for the support they provided in generating DNA methylome sequence data and Antoni Palusiński for photography expertise.

Tables

Table 1. Summary of half-time recoveries ($T_{1/2}$) and percentages of mobile fraction (Mf) for histone-GFP constructs measured in control and low light conditions

		$T_{1/2}$ [s]				Mf [%]			
Treatment	*Histone*	*Root*	*Hypocotyl*	*Meristem*	*Leaf*	*Root*	*Hypocotyl*	*Meristem*	*Leaf*
Control	H1.1	12.2 ± 0.8 (2)	6.2 ± 0.6 (2)	16.2 ± 1.3 (4)	6.8 ± 0.5 (7)	73.9% ± 1.9% (2)	91.1% ± 3.4% (2)	63.7% ± 2.0% (4)	86.1% ± 2.4% (7)
	H1.2	21.3 ± 1.8 (10)	21.1 ± 1.3 (7)	22.3 ± 4.0 (4)	16.8 ± 1.2 (9)	43.0% ± 1.5% (10)	77.9% ± 2.0% (7)	29.5% ± 2.2% (4)	72.3% ± 2.0% (9)
	H1.3	-	-	-	3.4 ± 0.3 (11)	-	-	-	97.1% ± 3.4% (11)
	H2B	25.7 ± 4.4 (6)	23.5 ± 5.2 (6)	13.1 ± 2.6 (10)	14.8 ± 1.9 (4)	64.8% ± 5.0% (6)	35.3% ± 3.4% (6)	38.5% ± 2.7% (10)	23.1% ± 1.1% (4)
Stress	H1.1	10.3 ± 0.8 (11)	8.5 ± 0.5 (8)	15.2 ± 0.8 (10)	8.4 ± 0.5 (5)	72.4% ± 2.0% (11)	86.0% ± 1.9% (8)	71.1% ± 1.4% (10)	86.3% ± 2.1% (5)
	H1.2	15.6 ± 1.0 (10)	15.1 ± 0.6 (5)	14.8 ± 2.2 (7)	19.4 ± 1.3 (6)	73.3% ± 1.7% (10)	80.2% ± 1.2% (5)	23.1% ± 1.2% (7)	74.4% ± 2.0% (6)
	H1.3	2 ± 0.3 (10)	1.3 ± 0.2 (6)	1.0 ± 0.1 (5)	3.0 ± 0.2 (13)	99.7% ± 6.7% (10)	100.0% ± 10.0% (6)	99.8% ± 10.7% (5)	100.0% ± 2.6% (13)
	H2B	24.9 ± 4.2 (10)	12.2 ± 0.8 (6)	29.4 ± 5.1 (9)	23.6 ± 3.1 (5)	48.6% ± 3.7% (10)	33.3% ± 0.8% (6)	47.3% ± 4.0% (9)	47.4% ± 2.7% (5)

$T_{1/2}$ and Mf were calculated based on estimation of parameters of the adopted FRAP model (see Materials and Methods). For each plant organ, histone dynamics were measured in control and stress conditions. All values are averages of at least 4 sets of single-cell FRAP data (the number of cells is shown in parentheses). High and low values of $T_{1/2}$ indicate low and high protein mobility, respectively. Mf indicates % of total protein pool not involved in stable interactions with chromatin. The presented values reflect characteristics of histone mobility during the first 70 seconds of the experiment. For histones whose fluorescence intensity does not reach a plateau within 70 s (Fig. 4A), extending the time of measurement could result in higher $T_{1/2}$ and lower mobile fraction estimates.

Figure legends

Figure 1. H1.3 is induced by prolonged low light treatment in an ABA-dependent manner.

(A) Distribution of Arabidopsis H1s in different tissues shown by green fluorescence of GFP-tagged forms. The locations of H1.1, H1.2 and H1.3 fusion proteins are shown in control conditions, while the H1.3 protein distribution is also shown after 4 days of low light treatment. Scale bars – 10 μm. **(B)** Relative expression (RT-qPCR) of *H1*s in wild-type (WT^{Ler}) plants in control conditions and after low light treatment (expression of *H1.3* in WT under normal conditions = 1). The plotted values are the means ± SD for replicates consisting of 4 plants grown in soil. **(C)** Relative expression of *H1.3* during growth in low light for 4 days followed by transfer back to control conditions. Yellow bar – control conditions, gray bar – low light period. The plotted values are the means ± SD for replicates consisting of ca. 35 plants grown in MS agar plates. **(D)** Relative expression of *H1.3* in *aba1* plants after 4 days of low light treatment. The plotted values are the means ± SD for replicates consisting of 4 plants grown in soil. All qRT-PCR measurements were normalized to the expression of *UBC*.

Figure 2. H1.3 influences stomatal functioning and biogenesis.

Effect of a lack of H1.3 on **(A)** CO_2 net assimilation rate (Pn) and **(B)** stomatal density (SD); the differences between Pn and SD values marked with different letters are statistically significant (p-value<0.05, Tukey's HSD test). **(C)** Expression of genes specific for guard cells in *h1.3*. Color bars indicate the percentage of genes showing altered (blue) or unchanged (light blue) expression in *h1.3,* divided into two different classes: preferentially expressed only in guard cells (n=61) and all expressed in guard cells (n=1063), classified as previously described (Leonhardt et al., 2004). The following criteria were met by all affected genes in *h1.3*: Fch>1.5 and p<0.05. **(D)** Relative expression (RT-qPCR) of genes with key functions in guard cell biogenesis in *h1.3* mutant and wild-type plants. All qRT-PCR measurements were performed for at least three replicates and were normalized to the expression of *UBC*.

Figure 3. H1.3 plays a critical role in developmental and physiological responses of Arabidopsis to environmental stresses.

(A) Relative expression of *H1*.3 (RT-qPCR) after 17 days of low light, drought and drought in low light conditions. RT-qPCR measurements were performed for at least three replicates and

were normalized to the expression of *UBC*. Effect of low light/drought treatment on **(B)** relative leaf water content (RWC), **(C)** absolute leaf water content (WC). The differences between RWC and WC values marked with different letters are statistically significant ($p<0.05$, Tukey's HSD test). **(D)** Diagrammatic representation of the phenotype (adult plant morphology and size) in control conditions and in response to drought under limited light conditions, of the wild-type (WT^{Ler}), *h1.3* and complemented *h1.3* mutant *(h1.3/*H1.3*)*. Scale bar for stem – 1 cm, scale square for plant area – 1 cm^2. **(E)** Venn diagram showing the number of genes with altered expression in response to low light/drought conditions in the wild-type (WT^{Ler}, red), *h1.3* (blue), and in both genotypes (yellow). The expression pattern of selected genes was verified by RT-qPCR (Supplemental Figs. S9 and S10).

Figure 4. Main and stress-inducible H1s have different *in vivo* chromatin binding properties.

FRAP analyses of GFP-tagged H1 variants and H2B in guard cells of unstressed plants. The data show the % of fluorescence recovery from 0 to 70 seconds after photobleaching. Note that 70 sec does not encompass the full recovery of the fluorescence for H1.1, H1.2 and H2B. Errors bars indicate ± SD (n = 7, 9, 11 and 4 nuclei, for H1.1, H1.2, H1.3 and H2B, respectively).

Figure 5. Genomic distribution of H1 variants.

(A) Genomic profiles of H1.2 and H1.3 in control conditions and after 4 days of low light (LL) treatment. The length of the colored bars represents enrichment or depletion compared with the total genome signal. H1.1 has a similar profile to H1.2 (Supplemental Fig. S15). Only the depletion of H1s in intergenic regions and enrichment in 3'UTRs are not statistically significant (Table S3). Asterisks indicate a significant difference between H1.2 occupancy in control and low light conditions, and between H1.2 and H1.3 in low light conditions. **(B)** Average distribution of the main H1 variants, H1.3 and H3 in control and low light conditions around the 3' and 5' ends (+/- 1kb) of transposons located in heterochromatin and euchromatin (differentiated by the level of H3K9me2 occupancy).

Figure 6. Distribution of H1s and H3 within genes according to their level of transcription in control conditions and low light.

The signal for histone occupancy was plotted for 1 kb around both the 5' (TSS) and 3' ends for five classes of genes divided according to their expression level.

Figure 7. Occupancy of linker histone variants in the Arabidopsis genome.

(A) H1 occupancies in low light observed in 5 kb around the TSS for a group of 4495 genes with the highest and 5999 genes with the lowest level of H3K4me3. **(B)** H1.3 distribution among genes divided according to the level of H3K4me3. **(C)** H1.3 distribution among genes divided according to the level of H3K9me2.

Figure 8. H1.3 is required for *de novo* DNA methylation in response to low light/drought.

(A) Averaged DNA methylation level in the CG, CHG and CHH contexts in wild-type (WT^{Ler}) and *h1.3* Arabidopsis in control and in low light/drought conditions (stress). Asterisks indicate level of significance: *** $p<10^{-256}$, ** $p<10^{-30}$, * $p<10^{-10}$ (T-test). **(B)** Patterns of DNA methylation (in the CG, CHG and CHH contexts) in regions that are hypermethylated in response to stress, for wild-type (WT^{Ler}) and *h1.3* plants in control and in low light/drought conditions. Averaged methylation (within a sliding 50-bp window) was plotted for 300 bp around both the start and the end of the regions.

Supplementary Material Legends

Figures S1-S21

Tables S1-S7

Datasets S1-S5

Videos S1-S3

Supplementary figures

Figure S1. Characterization of *H1.3* expression.

Figure S2. Expression analysis of Arabidopsis H1 with microarray data (AtGeneExpression, (Kilian et al., 2007)).

Figure S3. Schematic representation of the promoter regions of genes encoding Arabidopsis histone H1 somatic variants.

Figure S4. Characterization of the *h1.3* mutant line.

Figure S5. Stomatal density (SD) in leaves of wild-type (WT^{Ler}) and *h1.3* mutant plants grown in control and drought/low light conditions.

Figure S6. Growth of *h1.3* mutant plants is not restricted in response to low light/drought treatment unlike that of wild-type plants.

Figure S7. The *h1.3* mutant complemented with H1.3-GFP responds to combined low light/drought treatment similarly to wild-type plants.

Figure S8. ABA content in wild-type (WT^{Ler}) and *h1.3* plants in control and combined low light/drought conditions.

Figure S9. Verification by RT-qPCR of gene expression data obtained in microarray experiments examining the effects of combined low light/drought treatment (stress).

Figure S10. Verification by RT-qPCR of gene expression data obtained in microarray experiments examining the effects of combined low light/drought treatment (stress).

Figure S11. Moving sum plot of net charge for the C-terminal region of Arabidopsis histone H1 variants.

Figure S12. Phylogenetic tree of 196 plant H1 proteins with HMG sequences used as an outgroup.

Figure S13. Phylogenetic tree of 274 plant H1 proteins with *Dictyostelium discoideum* H1 protein as an outgroup.

Figure S14. CLANS clustering of 274 plant H1 proteins and a 2D image of the clustering results for an interactive graphical representation of *Viridiplantae* H1 sequences.

Figure S15. Genomic profiles for H1 variants in plants grown in control and 4-day low light (LL) conditions.

Figure S16. Distribution of H1 variants along Arabidopsis chromosome 1 in control and low light conditions.

Figure S17. Distribution of the main H1s and H3 within genes with different levels of H3K4me3 of plants grown in control and 4-day low light conditions.

Figure S18. Distribution of the main H1s and H3 within genes with different levels of H3K9me2 of plants grown in control and 4-day low light conditions.

Figure S19. Methylation levels in the triple *h1.1h1.2h1.3* mutant.

Figure S20. Methylation changes in response to stress in wild-type (WT^{Ler}) and *h1.3* mutant plants.

Figure S21. Global methylation changes in the *h1.3* mutant.

Figure S22. Arabidopsis linker histones belong to two structurally and functionally diversified families.

Supplementary tables

Table S1. Growth analysis and physiological parameters of wild-type (WT^{Ler}) and *h1.3* plants in the early-growth phase experiment.

Table S2. Growth analysis and physiological parameters of wild-type (WT^{Ler}) and *h1.3* plants, and the *h1.3* mutant complemented with H1.3-GFP (*h1.3*/H1.3) in the late-growth phase experiment.

Table S3. Statistics for H1 enrichment and depletion at genic features.

Table S4. Statistics for changes in methylation of euchromatic and heterochromatic transposable elements (TEs).

Table S5. Statistics for changes in methylation of euchromatic and heterochromatic genes.

Table S6. Statistics (T-test) for differences in the average global methylation level between genotypes and conditions in three different DNA methylation contexts.

Table S7. Sequences of oligonucleotide primers used in this study.

Supplementary datasets

Dataset S1. In a separate file. Genes with expression changed in *h1.3* mutant plants in control conditions, comparison with wild-type (WT^{Ler}) plants in control conditions, and GO analysis with AgriGO tool (Du et al., 2010).

Dataset S2. In a separate file. Genes with expression changed in wild-type (WT^{Ler}) plants in low light/drought conditions, comparison with wild-type (WT^{Ler}) plants in control conditions, and GO analysis with AgriGO tool (Du et al., 2010).

Dataset S3. In a separate file. Genes with expression changed in *h1.3* mutant plants in low light/drought conditions, comparison with *h1.3* mutant plants in control conditions, and GO analysis with AgriGO tool (Du et al., 2010).

Dataset S4. In a separate file. Genes with expression changed in *h1.3* mutant plants in low light/drought, comparison with wild-type (WT^{Ler}) plants in low light/drought conditions, and GO analysis with AgriGO tool (Du et al., 2010).

Dataset S5. In a separate file. Regions and genes which are occupied by H1.3 in control conditions.

Supplementary videos

Video S1. The dynamics of H1.1-GFP in guard cells during a FRAP experiment.

Video S2. The dynamics of H1.2-GFP in guard cells during a FRAP experiment.

Video S3. The dynamics of H1.3-GFP in guard cells during a FRAP experiment.

References

ALTSCHUL, S. F., MADDEN, T. L., SCHAFFER, A. A., ZHANG, J., ZHANG, Z., MILLER, W. & LIPMAN, D. J. 1997. Gapped BLAST and PSI-BLAST: a new generation of protein database search programs. *Nucleic Acids Res,* 25**,** 3389-402.

ANISIMOVA, M. & GASCUEL, O. 2006. Approximate likelihood-ratio test for branches: A fast, accurate, and powerful alternative. *Syst Biol,* 55**,** 539-52.

ARABIDOPSIS GENOME, I. 2000. Analysis of the genome sequence of the flowering plant Arabidopsis thaliana. *Nature,* 408**,** 796-815.

ASCENZI, R. & GANTT, J. S. 1997. A drought-stress-inducible histone gene in Arabidopsis thaliana is a member of a distinct class of plant linker histone variants. *Plant Mol Biol,* 34**,** 629-41.

ASCENZI, R. & GANTT, J. S. 1999a. Molecular genetic analysis of the drought-inducible linker histone variant in Arabidopsis thaliana. *Plant Mol Biol,* 41**,** 159-69.

ASCENZI, R. & GANTT, J. S. 1999b. Subnuclear distribution of the entire complement of linker histone variants in Arabidopsis thaliana. *Chromosoma,* 108**,** 345-55.

BANAS, A. K., LABUZ, J., SZTATELMAN, O., GABRYS, H. & FIEDOR, L. 2011. Expression of enzymes involved in chlorophyll catabolism in Arabidopsis is light controlled. *Plant Physiol,* 157**,** 1497-504.

BAUER, H., ACHE, P., LAUTNER, S., FROMM, J., HARTUNG, W., AL-RASHEID, K. A., SONNEWALD, S., SONNEWALD, U., KNEITZ, S., LACHMANN, N., MENDEL, R. R., BITTNER, F., HETHERINGTON, A. M. & HEDRICH, R. 2013. The stomatal response to reduced relative humidity requires guard cell-autonomous ABA synthesis. *Curr Biol,* 23**,** 53-7.

BERENDZEN, S. M., CAREY, J. D. & SMITH, E. B. 2006. Diltiazem-associated photodistributed hyperpigmentation in an elderly Hispanic female. *Int J Dermatol,* 45**,** 1450-2.

BILGER, W. & BJORKMAN, O. 1991. Temperature dependence of violaxanthin de-epoxidation and non-photochemical fluorescence quenching in intact leaves of Gossypium hirsutum L. and Malva parviflora L. *Planta,* 184**,** 226-34.

BRAUNSCHWEIG, U., HOGAN, G. J., PAGIE, L. & VAN STEENSEL, B. 2009. Histone H1 binding is inhibited by histone variant H3.3. *EMBO J,* 28**,** 3635-45.

BROWN, D. T., IZARD, T. & MISTELI, T. 2006. Mapping the interaction surface of linker histone H1(0) with the nucleosome of native chromatin in vivo. *Nat Struct Mol Biol,* 13**,** 250-5.

BRZESKI, J. & JERZMANOWSKI, A. 2003. Deficient in DNA methylation 1 (DDM1) defines a novel family of chromatin-remodeling factors. *J Biol Chem,* 278**,** 823-8.

CAO, K., LAILLER, N., ZHANG, Y., KUMAR, A., UPPAL, K., LIU, Z., LEE, E. K., WU, H., MEDRZYCKI, M., PAN, C., HO, P. Y., COOPER, G. P., JR., DONG, X., BOCK, C., BOUHASSIRA, E. E. & FAN, Y. 2013. High-resolution mapping of h1 linker histone variants in embryonic stem cells. *PLoS Genet,* 9**,** e1003417.

CAPELLA-GUTIERREZ, S., SILLA-MARTINEZ, J. M. & GABALDON, T. 2009. trimAl: a tool for automated alignment trimming in large-scale phylogenetic analyses. *Bioinformatics,* 25**,** 1972-3.

CATEZ, F., UEDA, T. & BUSTIN, M. 2006. Determinants of histone H1 mobility and chromatin binding in living cells. *Nat Struct Mol Biol,* 13**,** 305-10.

CATEZ, F., YANG, H., TRACEY, K. J., REEVES, R., MISTELI, T. & BUSTIN, M. 2004. Network of dynamic interactions between histone H1 and high-mobility-group proteins in chromatin. *Mol Cell Biol,* 24**,** 4321-8.

CHAVES, M. M., FLEXAS, J. & PINHEIRO, C. 2009. Photosynthesis under drought and salt stress: regulation mechanisms from whole plant to cell. *Ann Bot,* 103**,** 551-60.

CHRISTOPHOROU, M. A., CASTELO-BRANCO, G., HALLEY-STOTT, R. P., OLIVEIRA, C. S., LOOS, R., RADZISHEUSKAYA, A., MOWEN, K. A., BERTONE, P., SILVA, J. C., ZERNICKA-GOETZ, M., NIELSEN, M. L., GURDON, J. B. & KOUZARIDES, T. 2014. Citrullination regulates pluripotency and histone H1 binding to chromatin. *Nature,* 507**,** 104-8.

CLOUGH, S. J. & BENT, A. F. 1998. Floral dip: a simplified method for Agrobacterium-mediated transformation of Arabidopsis thaliana. *Plant J,* 16**,** 735-43.

COHEN, A. & BRAY, E. A. 1990. Characterization of three mRNAs that accumulate in wilted tomato leaves in response to elevated levels of endogenous abscisic acid. *Planta,* 182**,** 27-33.

COHEN, A., PLANT, A. L., MOSES, M. S. & BRAY, E. A. 1991. Organ-Specific and Environmentally Regulated Expression of Two Abscisic Acid-Induced Genes of Tomato : Nucleotide Sequence and Analysis of the Corresponding cDNAs. *Plant Physiol,* 97**,** 1367-74.

COLANERI, A. C. & JONES, A. M. 2013. Genome-wide quantitative identification of DNA differentially methylated sites in Arabidopsis seedlings growing at different water potential. *PLoS One,* 8**,** e59878.

CROOKS, G. E., HON, G., CHANDONIA, J. M. & BRENNER, S. E. 2004. WebLogo: a sequence logo generator. *Genome Res,* 14**,** 1188-90.

DOHENY-ADAMS, T., HUNT, L., FRANKS, P. J., BEERLING, D. J. & GRAY, J. E. 2012. Genetic manipulation of stomatal density influences stomatal size, plant growth and tolerance to restricted water supply across a growth carbon dioxide gradient. *Philos Trans R Soc Lond B Biol Sci,* 367**,** 547-55.

DU, Z., ZHOU, X., LING, Y., ZHANG, Z. & SU, Z. 2010. agriGO: a GO analysis toolkit for the agricultural community. *Nucleic Acids Res,* 38**,** W64-70.

DUBAS, E., JANOWIAK, F., KRZEWSKA, M., HURA, T. & ZUR, I. 2013. Endogenous ABA concentration and cytoplasmic membrane fluidity in microspores of oilseed rape (Brassica napus L.) genotypes differing in responsiveness to androgenesis induction. *Plant Cell Rep,* 32**,** 1465-75.

FAN, Y., NIKITINA, T., ZHAO, J., FLEURY, T. J., BHATTACHARYYA, R., BOUHASSIRA, E. E., STEIN, A., WOODCOCK, C. L. & SKOULTCHI, A. I. 2005. Histone H1 depletion in mammals alters global chromatin structure but causes specific changes in gene regulation. *Cell,* 123**,** 1199-212.

FEY, V., WAGNER, R., BRAUTIGAM, K. & PFANNSCHMIDT, T. 2005. Photosynthetic redox control of nuclear gene expression. *J Exp Bot,* 56**,** 1491-8.

FRICKEY, T. & LUPAS, A. 2004. CLANS: a Java application for visualizing protein families based on pairwise similarity. *Bioinformatics,* 20**,** 3702-4.

FUJITA, Y., FUJITA, M., SHINOZAKI, K. & YAMAGUCHI-SHINOZAKI, K. 2011. ABA-mediated transcriptional regulation in response to osmotic stress in plants. *J Plant Res,* 124**,** 509-25.
GENTY, B., BRIANTAIS, J.-M. & BAKER, N. R. 1989. The relationship between the quantum yield of photosynthetic electron transport and quenching of chlorophyll fluorescence. *Biochimica et Biophysica Acta (BBA) - General Subjects,* 990**,** 87-92.
GINALSKI, K., ELOFSSON, A., FISCHER, D. & RYCHLEWSKI, L. 2003. 3D-Jury: a simple approach to improve protein structure predictions. *Bioinformatics,* 19**,** 1015-8.
GINALSKI, K. & RYCHLEWSKI, L. 2003. Protein structure prediction of CASP5 comparative modeling and fold recognition targets using consensus alignment approach and 3D assessment. *Proteins,* 53 Suppl 6**,** 410-7.
GINALSKI, K., VON GROTTHUSS, M., GRISHIN, N. V. & RYCHLEWSKI, L. 2004. Detecting distant homology with Meta-BASIC. *Nucleic Acids Res,* 32**,** W576-81.
GLASSER, C., HABERER, G., FINKEMEIER, I., PFANNSCHMIDT, T., KLEINE, T., LEISTER, D., DIETZ, K. J., HAUSLER, R. E., GRIMM, B. & MAYER, K. F. 2014. Meta-analysis of retrograde signaling in Arabidopsis thaliana reveals a core module of genes embedded in complex cellular signaling networks. *Mol Plant,* 7**,** 1167-90.
GOMEZ-PORRAS, J. L., RIANO-PACHON, D. M., DREYER, I., MAYER, J. E. & MUELLER-ROEBER, B. 2007. Genome-wide analysis of ABA-responsive elements ABRE and CE3 reveals divergent patterns in Arabidopsis and rice. *BMC Genomics,* 8**,** 260.
GUINDON, S., DUFAYARD, J. F., LEFORT, V., ANISIMOVA, M., HORDIJK, W. & GASCUEL, O. 2010. New algorithms and methods to estimate maximum-likelihood phylogenies: assessing the performance of PhyML 3.0. *Syst Biol,* 59**,** 307-21.
GUO, L., ZHOU, J., ELLING, A. A., CHARRON, J. B. & DENG, X. W. 2008. Histone modifications and expression of light-regulated genes in Arabidopsis are cooperatively influenced by changing light conditions. *Plant Physiol,* 147**,** 2070-83.
HARSHMAN, S. W., YOUNG, N. L., PARTHUN, M. R. & FREITAS, M. A. 2013. H1 histones: current perspectives and challenges. *Nucleic Acids Res,* 41**,** 9593-609.
IZZO, A., KAMIENIARZ-GDULA, K., RAMIREZ, F., NOUREEN, N., KIND, J., MANKE, T., VAN STEENSEL, B. & SCHNEIDER, R. 2013. The genomic landscape of the somatic linker histone subtypes H1.1 to H1.5 in human cells. *Cell Rep,* 3**,** 2142-54.
JEDDELOH, J. A., BENDER, J. & RICHARDS, E. J. 1998. The DNA methylation locus DDM1 is required for maintenance of gene silencing in Arabidopsis. *Genes Dev,* 12**,** 1714-25.
JERZMANOWSKI, A., PRZEWŁOKA, M. & GRASSER, K. D. 2000. Linker Histones and HMG1 Proteins of Higher Plants. *Plant Biology,* 2**,** 586-597.
JIANG, C. & PUGH, B. F. 2009. Nucleosome positioning and gene regulation: advances through genomics. *Nat Rev Genet,* 10**,** 161-72.
JIAO, Y., WICKETT, N. J., AYYAMPALAYAM, S., CHANDERBALI, A. S., LANDHERR, L., RALPH, P. E., TOMSHO, L. P., HU, Y., LIANG, H., SOLTIS, P. S., SOLTIS, D. E., CLIFTON, S. W., SCHLARBAUM, S. E., SCHUSTER, S. C., MA, H., LEEBENS-MACK, J. & DEPAMPHILIS, C. W. 2011. Ancestral polyploidy in seed plants and angiosperms. *Nature,* 473**,** 97-100.
JULLIEN, J., ASTRAND, C., HALLEY-STOTT, R. P., GARRETT, N. & GURDON, J. B. 2010. Characterization of somatic cell nuclear reprogramming by oocytes in which a

linker histone is required for pluripotency gene reactivation. *Proc Natl Acad Sci U S A,* 107**,** 5483-8.
KATOH, K. & STANDLEY, D. M. 2013. MAFFT multiple sequence alignment software version 7: improvements in performance and usability. *Mol Biol Evol,* 30**,** 772-80.
KHANDELWAL, A., ELVITIGALA, T., GHOSH, B. & QUATRANO, R. S. 2008. Arabidopsis transcriptome reveals control circuits regulating redox homeostasis and the role of an AP2 transcription factor. *Plant Physiol,* 148**,** 2050-8.
KILIAN, J., WHITEHEAD, D., HORAK, J., WANKE, D., WEINL, S., BATISTIC, O., D'ANGELO, C., BORNBERG-BAUER, E., KUDLA, J. & HARTER, K. 2007. The AtGenExpress global stress expression data set: protocols, evaluation and model data analysis of UV-B light, drought and cold stress responses. *Plant J,* 50**,** 347-63.
KINOSHITA, T. & SEKI, M. 2014. Epigenetic memory for stress response and adaptation in plants. *Plant Cell Physiol,* 55**,** 1859-63.
KLEPPER, B. & BARRS, H. D. 1968. Effects of salt secretion on psychrometric determinations of water potential of cotton leaves. *Plant Physiol,* 43**,** 1138-40.
KLUGHAMMER, C. & SCHREIBER, U. 1994. An improved method, using saturating light pulses, for the determination of photosystem I quantum yield via P700+-absorbance changes at 830 nm. *Planta,* 192**,** 261-268.
KRIVOV, G. G., SHAPOVALOV, M. V. & DUNBRACK, R. L., JR. 2009. Improved prediction of protein side-chain conformations with SCWRL4. *Proteins,* 77**,** 778-95.
KRUEGER, F. & ANDREWS, S. R. 2011. Bismark: a flexible aligner and methylation caller for Bisulfite-Seq applications. *Bioinformatics,* 27**,** 1571-2.
KUMARI, A., JEWARIA, P. K., BERGMANN, D. C. & KAKIMOTO, T. 2014. Arabidopsis reduces growth under osmotic stress by decreasing SPEECHLESS protein. *Plant Cell Physiol,* 55**,** 2037-46.
LAKE, J. A., QUICK, W. P., BEERLING, D. J. & WOODWARD, F. I. 2001. Plant development. Signals from mature to new leaves. *Nature,* 411**,** 154.
LAU, O. S. & BERGMANN, D. C. 2012. Stomatal development: a plant's perspective on cell polarity, cell fate transitions and intercellular communication. *Development,* 139**,** 3683-92.
LAUNHOLT, D., MERKLE, T., HOUBEN, A., SCHULZ, A. & GRASSER, K. D. 2006. Arabidopsis chromatin-associated HMGA and HMGB use different nuclear targeting signals and display highly dynamic localization within the nucleus. *Plant Cell,* 18**,** 2904-18.
LEONHARDT, N., KWAK, J. M., ROBERT, N., WANER, D., LEONHARDT, G. & SCHROEDER, J. I. 2004. Microarray expression analyses of Arabidopsis guard cells and isolation of a recessive abscisic acid hypersensitive protein phosphatase 2C mutant. *Plant Cell,* 16**,** 596-615.
LEPISTO, A., TOIVOLA, J., NIKKANEN, L. & RINTAMAKI, E. 2012. Retrograde signaling from functionally heterogeneous plastids. *Front Plant Sci,* 3**,** 286.
LETUNIC, I. & BORK, P. 2011. Interactive Tree Of Life v2: online annotation and display of phylogenetic trees made easy. *Nucleic Acids Res,* 39**,** W475-8.
LETUNIC, I., COPLEY, R. R., PILS, B., PINKERT, S., SCHULTZ, J. & BORK, P. 2006. SMART 5: domains in the context of genomes and networks. *Nucleic Acids Res,* 34**,** D257-60.

LIPPMAN, Z., GENDREL, A. V., BLACK, M., VAUGHN, M. W., DEDHIA, N., MCCOMBIE, W. R., LAVINE, K., MITTAL, V., MAY, B., KASSCHAU, K. D., CARRINGTON, J. C., DOERGE, R. W., COLOT, V. & MARTIENSSEN, R. 2004. Role of transposable elements in heterochromatin and epigenetic control. *Nature,* 430**,** 471-6.

LUO, C., SIDOTE, D. J., ZHANG, Y., KERSTETTER, R. A., MICHAEL, T. P. & LAM, E. 2012. Integrative analysis of chromatin states in Arabidopsis identified potential regulatory mechanisms for natural antisense transcript production. *Plant J.*

LUPAS, A., VAN DYKE, M. & STOCK, J. 1991. Predicting coiled coils from protein sequences. *Science,* 252**,** 1162-4.

MACALISTER, C. A., OHASHI-ITO, K. & BERGMANN, D. C. 2007. Transcription factor control of asymmetric cell divisions that establish the stomatal lineage. *Nature,* 445**,** 537-40.

MARCHLER-BAUER, A., LU, S., ANDERSON, J. B., CHITSAZ, F., DERBYSHIRE, M. K., DEWEESE-SCOTT, C., FONG, J. H., GEER, L. Y., GEER, R. C., GONZALES, N. R., GWADZ, M., HURWITZ, D. I., JACKSON, J. D., KE, Z., LANCZYCKI, C. J., LU, F., MARCHLER, G. H., MULLOKANDOV, M., OMELCHENKO, M. V., ROBERTSON, C. L., SONG, J. S., THANKI, N., YAMASHITA, R. A., ZHANG, D., ZHANG, N., ZHENG, C. & BRYANT, S. H. 2011. CDD: a Conserved Domain Database for the functional annotation of proteins. *Nucleic Acids Res,* 39**,** D225-9.

MCBRYANT, S. J., LU, X. & HANSEN, J. C. 2010. Multifunctionality of the linker histones: an emerging role for protein-protein interactions. *Cell Res,* 20**,** 519-28.

MOISSIARD, G., COKUS, S. J., CARY, J., FENG, S., BILLI, A. C., STROUD, H., HUSMANN, D., ZHAN, Y., LAJOIE, B. R., MCCORD, R. P., HALE, C. J., FENG, W., MICHAELS, S. D., FRAND, A. R., PELLEGRINI, M., DEKKER, J., KIM, J. K. & JACOBSEN, S. E. 2012. MORC family ATPases required for heterochromatin condensation and gene silencing. *Science,* 336**,** 1448-51.

MOTT, R. 2000. Accurate formula for P-values of gapped local sequence and profile alignments. *J Mol Biol,* 300**,** 649-59.

NEDBAL L., W., J. 2004. Chlorophyll fluorescence imaging of leaves and fruits. *Papageorgiou, G., Govindjee, editors. Chlorophyll fluorescence, a signature of photosynthesis, Dordrecht Springer***,** 389–407.

NELSON, J. D., DENISENKO, O., SOVA, P. & BOMSZTYK, K. 2006. Fast chromatin immunoprecipitation assay. *Nucleic Acids Res,* 34**,** e2.

NIELSEN, H., ENGELBRECHT, J., BRUNAK, S. & VON HEIJNE, G. 1997. Identification of prokaryotic and eukaryotic signal peptides and prediction of their cleavage sites. *Protein Eng,* 10**,** 1-6.

PARKINSON, K. J., DAY, W. & LEACH, J. E. 1980. A Portable System for Measuring the Photosynthesis and Transpiration of Graminaceous Leaves. *Journal of Experimental Botany,* 31**,** 1441-1453.

PEI, J., SADREYEV, R. & GRISHIN, N. V. 2003. PCMA: fast and accurate multiple sequence alignment based on profile consistency. *Bioinformatics,* 19**,** 427-8.

PEREZ-MONTERO, S., CARBONELL, A., MORAN, T., VAQUERO, A. & AZORIN, F. 2013. The embryonic linker histone H1 variant of Drosophila, dBigH1, regulates zygotic genome activation. *Dev Cell,* 26**,** 578-90.

PFALZ, J., LIEBERS, M., HIRTH, M., GRUBLER, B., HOLTZEGEL, U., SCHROTER, Y., DIETZEL, L. & PFANNSCHMIDT, T. 2012. Environmental control of plant nuclear gene expression by chloroplast redox signals. *Front Plant Sci,* 3**,** 257.

PHAIR, R. D., SCAFFIDI, P., ELBI, C., VECEROVA, J., DEY, A., OZATO, K., BROWN, D. T., HAGER, G., BUSTIN, M. & MISTELI, T. 2004. Global nature of dynamic protein-chromatin interactions in vivo: three-dimensional genome scanning and dynamic interaction networks of chromatin proteins. *Mol Cell Biol,* 24**,** 6393-402.

PLANT, A. L., COHEN, A., MOSES, M. S. & BRAY, E. A. 1991. Nucleotide sequence and spatial expression pattern of a drought- and abscisic Acid-induced gene of tomato. *Plant Physiol,* 97**,** 900-6.

PRZEWLOKA, M. R., WIERZBICKI, A. T., SLUSARCZYK, J., KURAS, M., GRASSER, K. D., STEMMER, C. & JERZMANOWSKI, A. 2002. The "drought-inducible" histone H1s of tobacco play no role in male sterility linked to alterations in H1 variants. *Planta,* 215**,** 371-9.

RAGHURAM, N., CARRERO, G., TH'NG, J. & HENDZEL, M. J. 2009. Molecular dynamics of histone H1. *Biochem Cell Biol,* 87**,** 189-206.

RAMAKRISHNAN, V., FINCH, J. T., GRAZIANO, V., LEE, P. L. & SWEET, R. M. 1993. Crystal structure of globular domain of histone H5 and its implications for nucleosome binding. *Nature,* 362**,** 219-23.

REA, M., ZHENG, W., CHEN, M., BRAUD, C., BHANGU, D., ROGNAN, T. N. & XIAO, W. 2012. Histone H1 affects gene imprinting and DNA methylation in Arabidopsis. *Plant J,* 71**,** 776-86.

REHRAUER, H., AQUINO, C., GRUISSEM, W., HENZ, S. R., HILSON, P., LAUBINGER, S., NAOUAR, N., PATRIGNANI, A., ROMBAUTS, S., SHU, H., VAN DE PEER, Y., VUYLSTEKE, M., WEIGEL, D., ZELLER, G. & HENNIG, L. 2010. AGRONOMICS1: a new resource for Arabidopsis transcriptome profiling. *Plant Physiol,* 152**,** 487-99.

ROSA, S., NTOUKAKIS, V., OHMIDO, N., PENDLE, A., ABRANCHES, R. & SHAW, P. 2014. Cell differentiation and development in Arabidopsis are associated with changes in histone dynamics at the single-cell level. *Plant Cell,* 26**,** 4821-33.

SALI, A. & BLUNDELL, T. L. 1993. Comparative protein modelling by satisfaction of spatial restraints. *J Mol Biol,* 234**,** 779-815.

SCHMID, M., DAVISON, T. S., HENZ, S. R., PAPE, U. J., DEMAR, M., VINGRON, M., SCHOLKOPF, B., WEIGEL, D. & LOHMANN, J. U. 2005. A gene expression map of Arabidopsis thaliana development. *Nat Genet,* 37**,** 501-6.

SCIPPA, G. S., DI MICHELE, M., ONELLI, E., PATRIGNANI, G., CHIATANTE, D. & BRAY, E. A. 2004. The histone-like protein H1-S and the response of tomato leaves to water deficit. *J Exp Bot,* 55**,** 99-109.

SCIPPA, G. S., GRIFFITHS, A., CHIATANTE, D. & BRAY, E. A. 2000. The H1 histone variant of tomato, H1-S, is targeted to the nucleus and accumulates in chromatin in response to water-deficit stress. *Planta,* 211**,** 173-81.

SHAHHOSEINI, M., FAVAEDI, R., BAHARVAND, H., SHARMA, V. & STUNNENBERG, H. G. 2010. Evidence for a dynamic role of the linker histone variant H1x during retinoic acid-induced differentiation of NT2 cells. *FEBS Lett,* 584**,** 4661-4.

SHE, W., GRIMANELLI, D., RUTOWICZ, K., WHITEHEAD, M. W., PUZIO, M., KOTLINSKI, M., JERZMANOWSKI, A. & BAROUX, C. 2013. Chromatin

reprogramming during the somatic-to-reproductive cell fate transition in plants. *Development,* 140**,** 4008-19.
SMITH, K. T. & WORKMAN, J. L. 2012. Chromatin proteins: key responders to stress. *PLoS Biol,* 10**,** e1001371.
STASEVICH, T. J., MUELLER, F., BROWN, D. T. & MCNALLY, J. G. 2010. Dissecting the binding mechanism of the linker histone in live cells: an integrated FRAP analysis. *EMBO J,* 29**,** 1225-34.
STRIZHOV, N., ABRAHAM, E., OKRESZ, L., BLICKLING, S., ZILBERSTEIN, A., SCHELL, J., KONCZ, C. & SZABADOS, L. 1997. Differential expression of two P5CS genes controlling proline accumulation during salt-stress requires ABA and is regulated by ABA1, ABI1 and AXR2 in Arabidopsis. *Plant J,* 12**,** 557-69.
TALBERT, P. B., AHMAD, K., ALMOUZNI, G., AUSIO, J., BERGER, F., BHALLA, P. L., BONNER, W. M., CANDE, W. Z., CHADWICK, B. P., CHAN, S. W., CROSS, G. A., CUI, L., DIMITROV, S. I., DOENECKE, D., EIRIN-LOPEZ, J. M., GOROVSKY, M. A., HAKE, S. B., HAMKALO, B. A., HOLEC, S., JACOBSEN, S. E., KAMIENIARZ, K., KHOCHBIN, S., LADURNER, A. G., LANDSMAN, D., LATHAM, J. A., LOPPIN, B., MALIK, H. S., MARZLUFF, W. F., PEHRSON, J. R., POSTBERG, J., SCHNEIDER, R., SINGH, M. B., SMITH, M. M., THOMPSON, E., TORRES-PADILLA, M. E., TREMETHICK, D. J., TURNER, B. M., WATERBORG, J. H., WOLLMANN, H., YELAGANDULA, R., ZHU, B. & HENIKOFF, S. 2012. A unified phylogeny-based nomenclature for histone variants. *Epigenetics Chromatin,* 5**,** 7.
VAN DIJK, K., DING, Y., MALKARAM, S., RIETHOVEN, J. J., LIU, R., YANG, J., LACZKO, P., CHEN, H., XIA, Y., LADUNGA, I., AVRAMOVA, Z. & FROMM, M. 2010. Dynamic changes in genome-wide histone H3 lysine 4 methylation patterns in response to dehydration stress in Arabidopsis thaliana. *BMC Plant Biol,* 10**,** 238.
VAN ZANTEN, M., TESSADORI, F., MCLOUGHLIN, F., SMITH, R., MILLENAAR, F. F., VAN DRIEL, R., VOESENEK, L. A., PEETERS, A. J. & FRANSZ, P. 2010. Photoreceptors CRYTOCHROME2 and phytochrome B control chromatin compaction in Arabidopsis. *Plant Physiol,* 154**,** 1686-96.
WEI, T. & O'CONNELL, M. A. 1996. Structure and characterization of a putative drought-inducible H1 histone gene. *Plant Mol Biol,* 30**,** 255-68.
WIERZBICKI, A. T. & JERZMANOWSKI, A. 2005. Suppression of histone H1 genes in Arabidopsis results in heritable developmental defects and stochastic changes in DNA methylation. *Genetics,* 169**,** 997-1008.
WOOTTON, J. C. 1994. Non-globular domains in protein sequences: automated segmentation using complexity measures. *Comput Chem,* 18**,** 269-85.
YANG, S. M., KIM, B. J., NORWOOD TORO, L. & SKOULTCHI, A. I. 2013. H1 linker histone promotes epigenetic silencing by regulating both DNA methylation and histone H3 methylation. *Proc Natl Acad Sci U S A,* 110**,** 1708-13.
ZEMACH, A., KIM, M. Y., HSIEH, P. H., COLEMAN-DERR, D., ESHED-WILLIAMS, L., THAO, K., HARMER, S. L. & ZILBERMAN, D. 2013. The Arabidopsis nucleosome remodeler DDM1 allows DNA methyltransferases to access H1-containing heterochromatin. *Cell,* 153**,** 193-205.
ZHANG, Y., COOKE, M., PANJWANI, S., CAO, K., KRAUTH, B., HO, P. Y., MEDRZYCKI, M., BERHE, D. T., PAN, C., MCDEVITT, T. C. & FAN, Y. 2012a. Histone h1 depletion impairs embryonic stem cell differentiation. *PLoS Genet,* 8**,** e1002691.

ZHANG, Z., LI, J., ZHAO, X. Q., WANG, J., WONG, G. K. & YU, J. 2006. KaKs_Calculator: calculating Ka and Ks through model selection and model averaging. *Genomics Proteomics Bioinformatics,* 4**,** 259-63.

ZHANG, Z., XIAO, J., WU, J., ZHANG, H., LIU, G., WANG, X. & DAI, L. 2012b. ParaAT: a parallel tool for constructing multiple protein-coding DNA alignments. *Biochem Biophys Res Commun,* 419**,** 779-81.

ZHOU, J., WANG, X., HE, K., CHARRON, J. B., ELLING, A. A. & DENG, X. W. 2010. Genome-wide profiling of histone H3 lysine 9 acetylation and dimethylation in Arabidopsis reveals correlation between multiple histone marks and gene expression. *Plant Mol Biol,* 72**,** 585-95.

ZIMMERMANN, P., HIRSCH-HOFFMANN, M., HENNIG, L. & GRUISSEM, W. 2004. GENEVESTIGATOR. Arabidopsis microarray database and analysis toolbox. *Plant Physiol,* 136**,** 2621-32.

ZONG, W., ZHONG, X., YOU, J. & XIONG, L. 2013. Genome-wide profiling of histone H3K4-tri-methylation and gene expression in rice under drought stress. *Plant Mol Biol,* 81**,** 175-88.

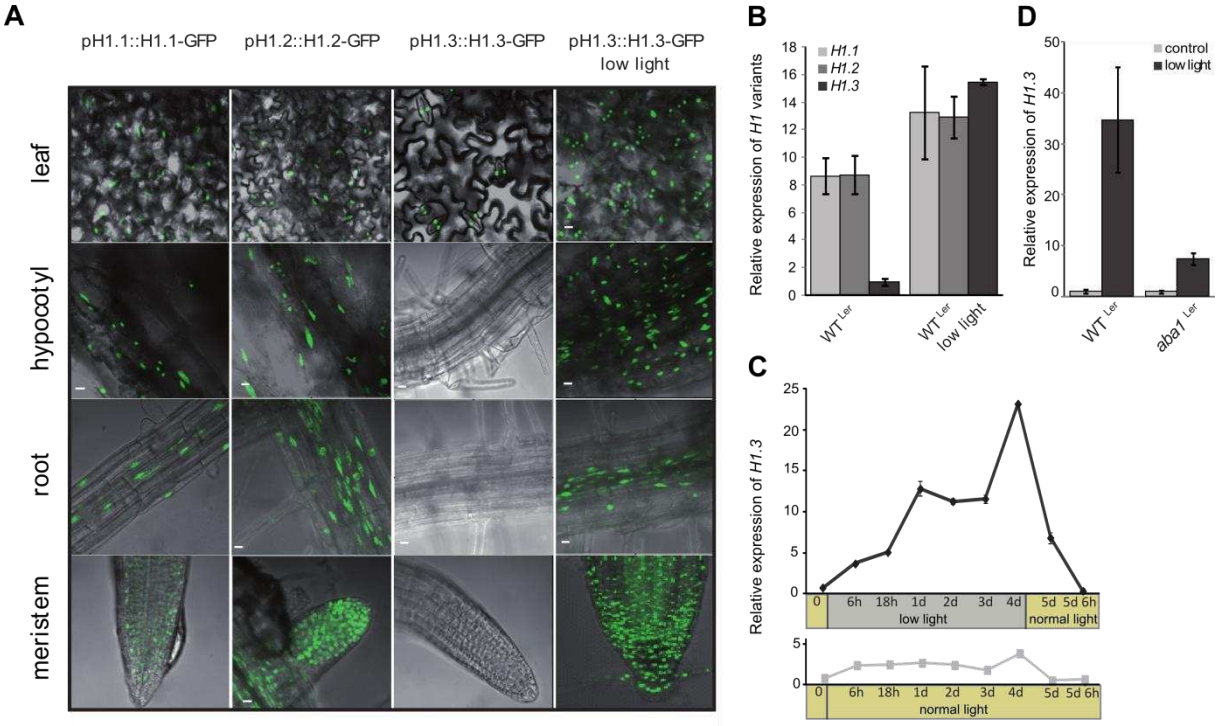

Figure 1. H1.3 is induced by prolonged low light treatment in an ABA-dependent manner.

(A) Distribution of Arabidopsis H1s in different tissues shown by green fluorescence of GFP-tagged forms. The locations of H1.1, H1.2 and H1.3 fusion proteins are shown in control conditions, while the H1.3 protein distribution is also shown after 4 days of low light treatment. Scale bars – 10 μm. **(B)** Relative expression (RT-qPCR) of *H1*s in wild-type (WT^{Ler}) plants in control conditions and after low light treatment (expression of *H1.3* in WT under normal conditions = 1). The plotted values are the means ± SD for replicates consisting of 4 plants grown in soil. **(C)** Relative expression of *H1.3* during growth in low light for 4 days followed by transfer back to control conditions. Yellow bar – control conditions, gray bar – low light period. The plotted values are the means ± SD for replicates consisting of ca. 35 plants grown in MS agar plates. **(D)** Relative expression of *H1.3* in *aba1* plants after 4 days of low light treatment. The plotted values are the means ± SD for replicates consisting of 4 plants grown in soil. All qRT-PCR measurements were normalized to the expression of *UBC*.

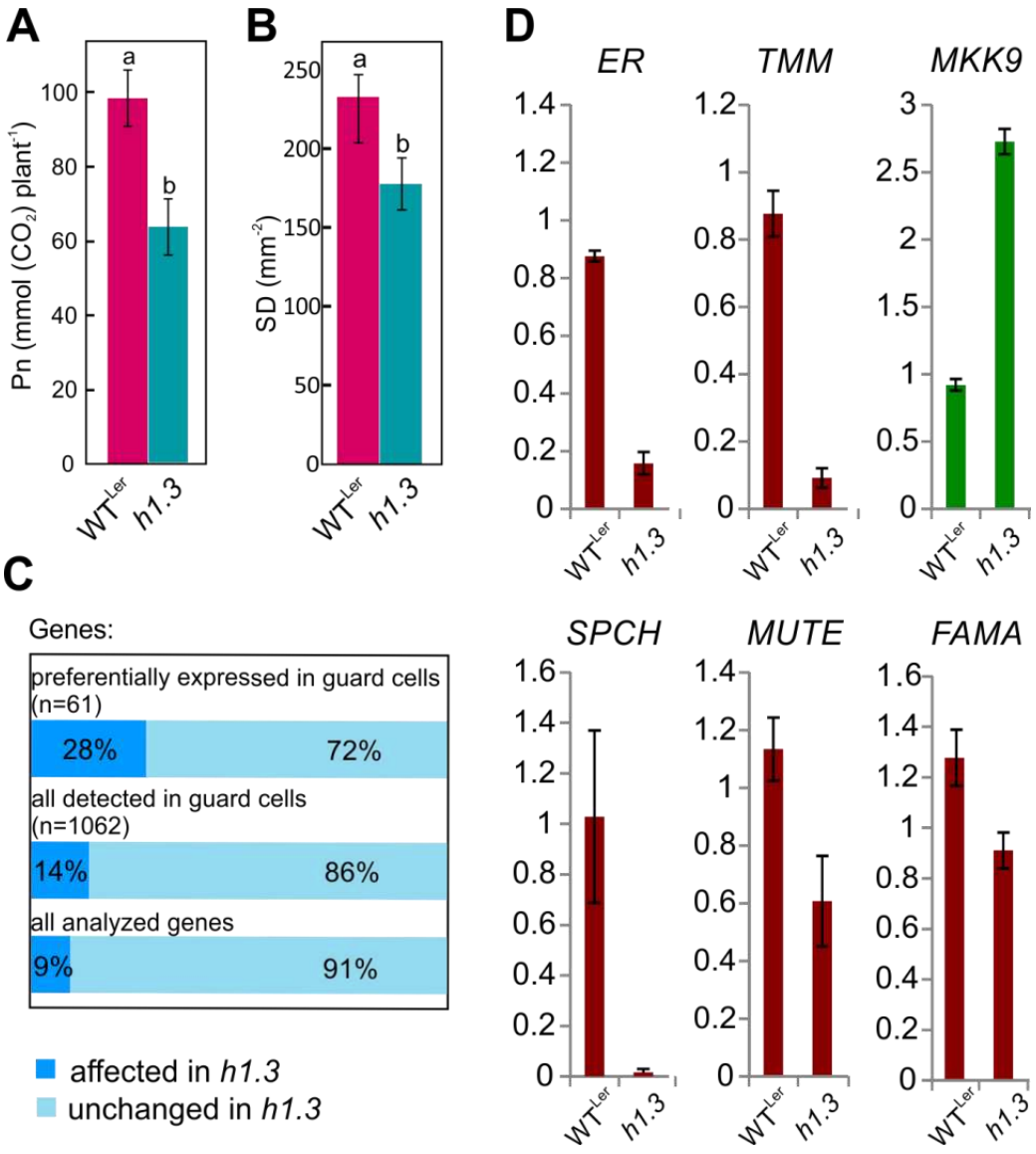

Figure 2. H1.3 influences stomatal functioning and biogenesis.

Effect of a lack of H1.3 on **(A)** CO_2 net assimilation rate (Pn) and **(B)** stomatal density (SD); the differences between Pn and SD values marked with different letters are statistically significant (p-value<0.05, Tukey's HSD test). **(C)** Expression of genes specific for guard cells in *h1.3*. Color bars indicate the percentage of genes showing altered (blue) or unchanged (light blue) expression in *h1.3,* divided into two different classes: preferentially expressed only in guard cells (n=61) and all expressed in guard cells (n=1063), classified as previously described (Leonhardt et al., 2004). The following criteria were met by all affected genes in *h1.3*: Fch>1.5 and p<0.05. **(D)** Relative expression (RT-qPCR) of genes with key functions in guard cell biogenesis in *h1.3* mutant and wild-type plants. All qRT-PCR measurements were performed for at least three replicates and were normalized to the expression of *UBC*.

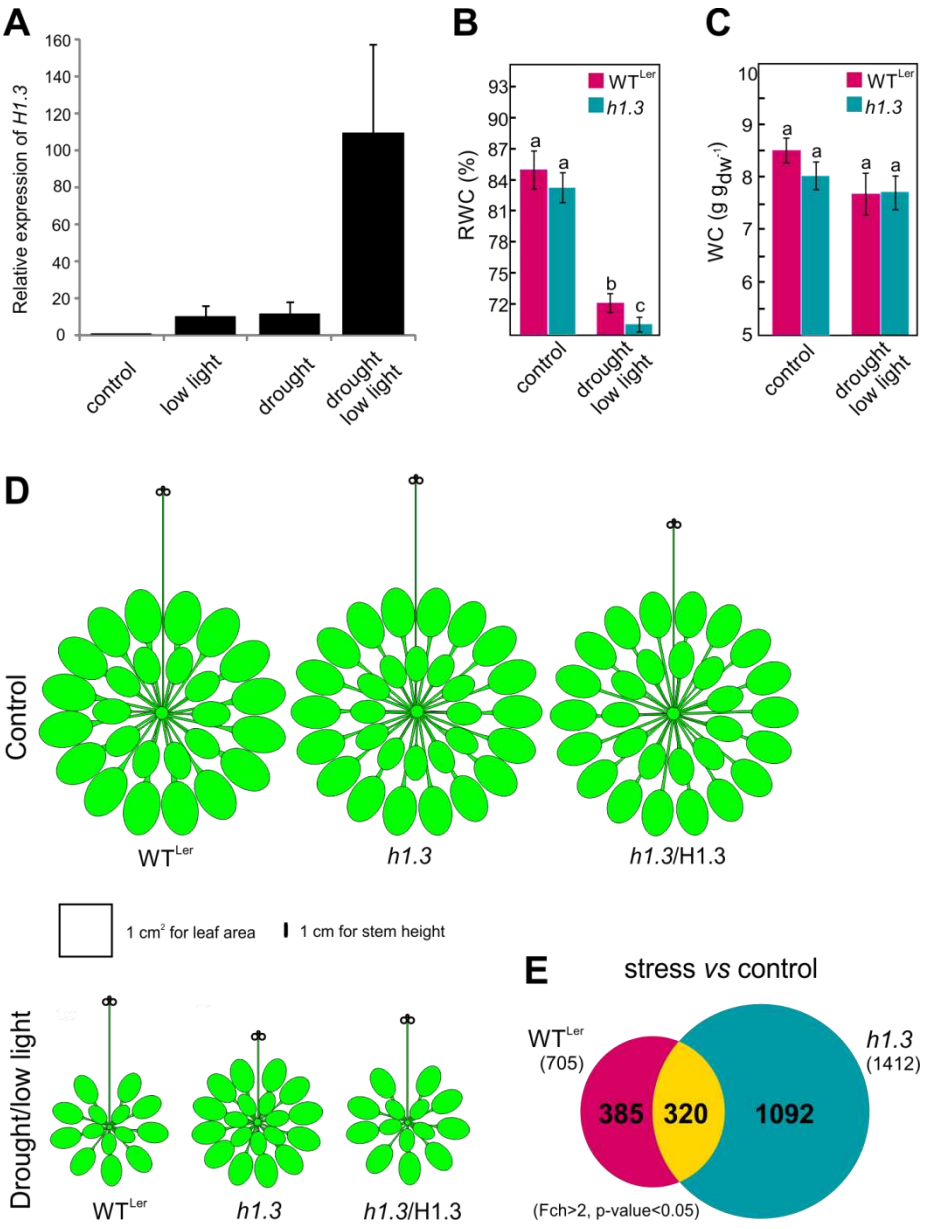

Figure 3. H1.3 plays a critical role in developmental and physiological responses of Arabidopsis to environmental stresses.

((A) Relative expression of *H1*.3 (RT-qPCR) after 17 days of low light, drought and drought in low light conditions. RT-qPCR measurements were performed for at least three replicates and were normalized to the expression of *UBC*. Effect of low light/drought treatment on **(B)** relative leaf water content (RWC), **(C)** absolute leaf water content (WC). The differences between RWC and WC values marked with different letters are statistically significant ($p<0.05$, Tukey's HSD test). **(D)** Diagrammatic representation of the phenotype (adult plant morphology and size) in control conditions and in response to drought under limited light conditions, of the wild-type (WT^{Ler}), *h1.3* and complemented *h1.3* mutant *(h1.3/*H1.3*)*. Scale

bar for stem – 1 cm, scale square for plant area – 1 cm^2. **(E)** Venn diagram showing the number of genes with altered expression in response to low light/drought conditions in the wild-type (WT^{Ler}, red), *h1.3* (blue), and in both genotypes (yellow). The expression pattern of selected genes was verified by RT-qPCR (Supplemental Figs. S9 and S10).

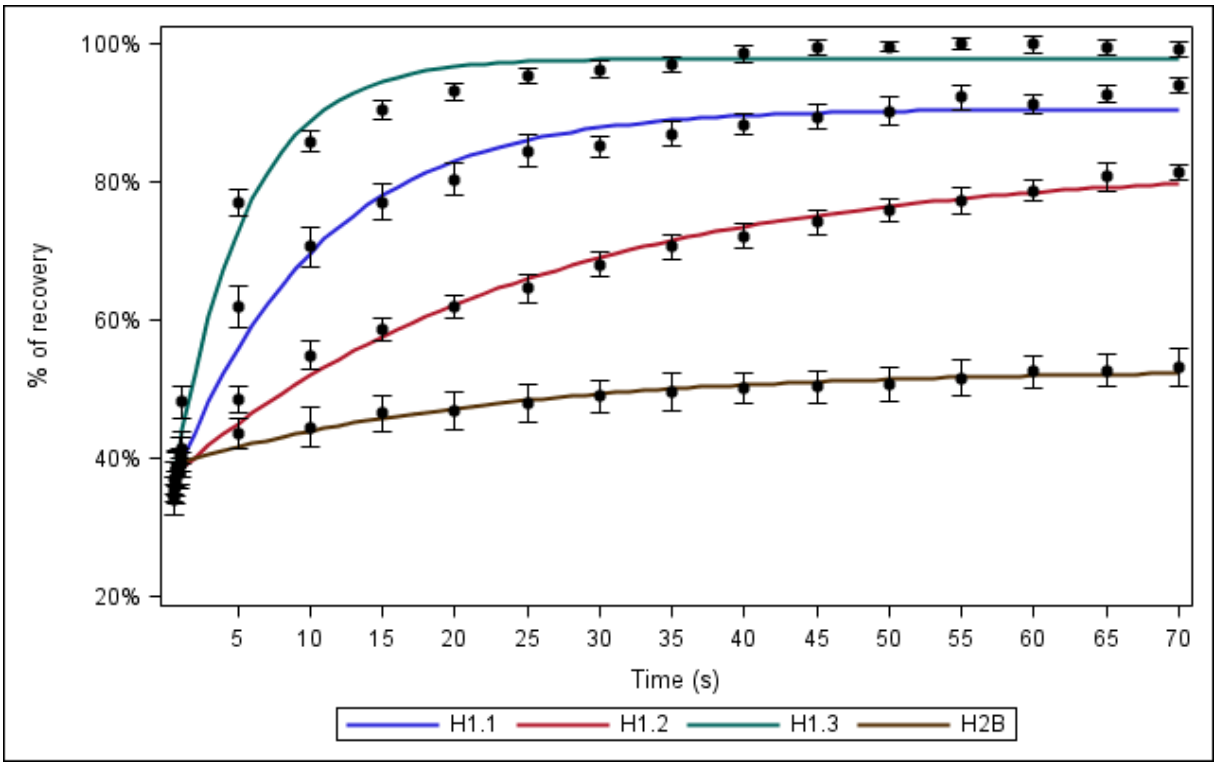

Figure 4. Main and stress-inducible H1s have different *in vivo* chromatin binding properties.

FRAP analyses of GFP-tagged H1 variants and H2B in guard cells of unstressed plants. The data show the % of fluorescence recovery from 0 to 70 seconds after photobleaching. Note that 70 sec does not encompass the full recovery of the fluorescence for H1.1, H1.2 and H2B. Errors bars indicate ± SD (n = 7, 9, 11 and 4 nuclei, for H1.1, H1.2, H1.3 and H2B, respectively).

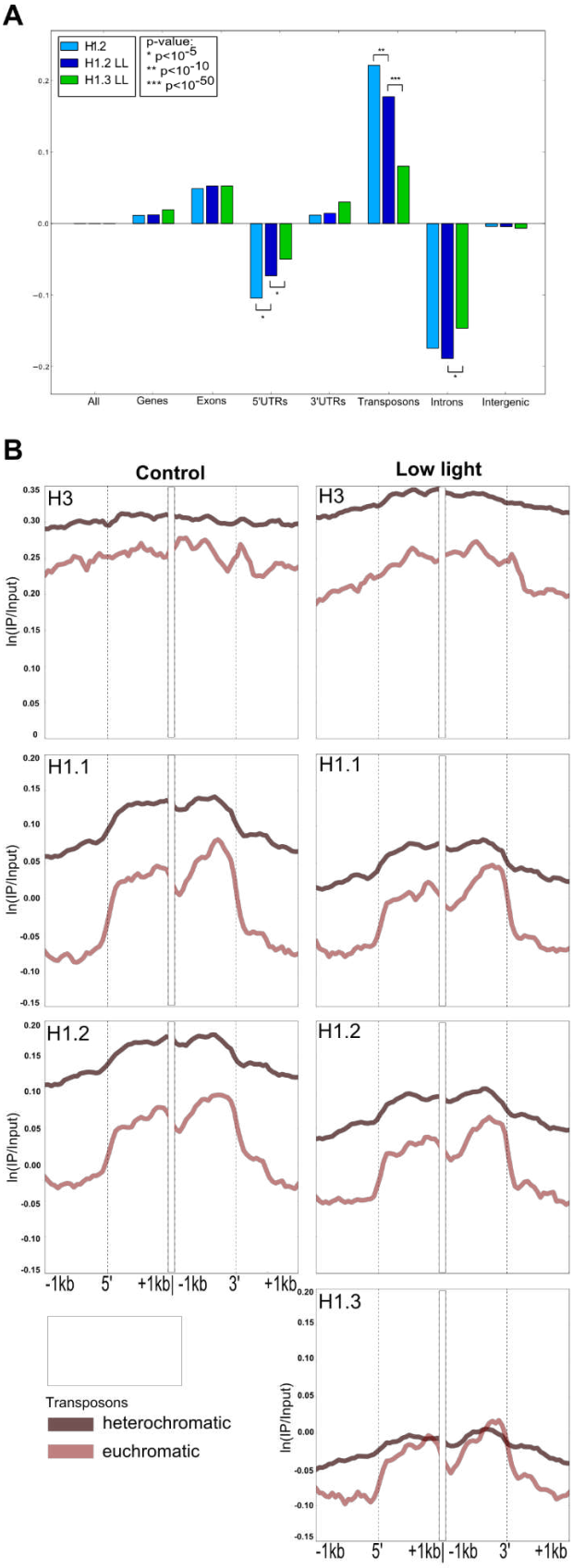
A
H1.2
H1.2 LL
H1.3 LL
p-value:
* p<10-5
** p<10-10
*** p<10-50
All
Genes
Exons
5'UTRs
3'UTRs
Transposons
Introns
Intergenic
B
Control
Low light
H3
H1.1
H1.2
H1.3
ln(IP/Input)
-1kb
5'
+1kb
-1kb
3'
+1kb
Transposons
heterochromatic
euchromatic

Figure 5. Genomic distribution of H1 variants.

(A) Genomic profiles of H1.2 and H1.3 in control conditions and after 4 days of low light (LL) treatment. The length of the colored bars represents enrichment or depletion compared with the total genome signal. H1.1 has a similar profile to H1.2 (Supplemental Fig. S15). Only the depletion of H1s in intergenic regions and enrichment in 3'UTRs are not statistically significant (Table S3). Asterisks indicate a significant difference between H1.2 occupancy in control and low light conditions, and between H1.2 and H1.3 in low light conditions. **(B)** Average distribution of the main H1 variants, H1.3 and H3 in control and low light conditions around the 3' and 5' ends (+/- 1kb) of transposons located in heterochromatin and euchromatin (differentiated by the level of H3K9me2 occupancy).

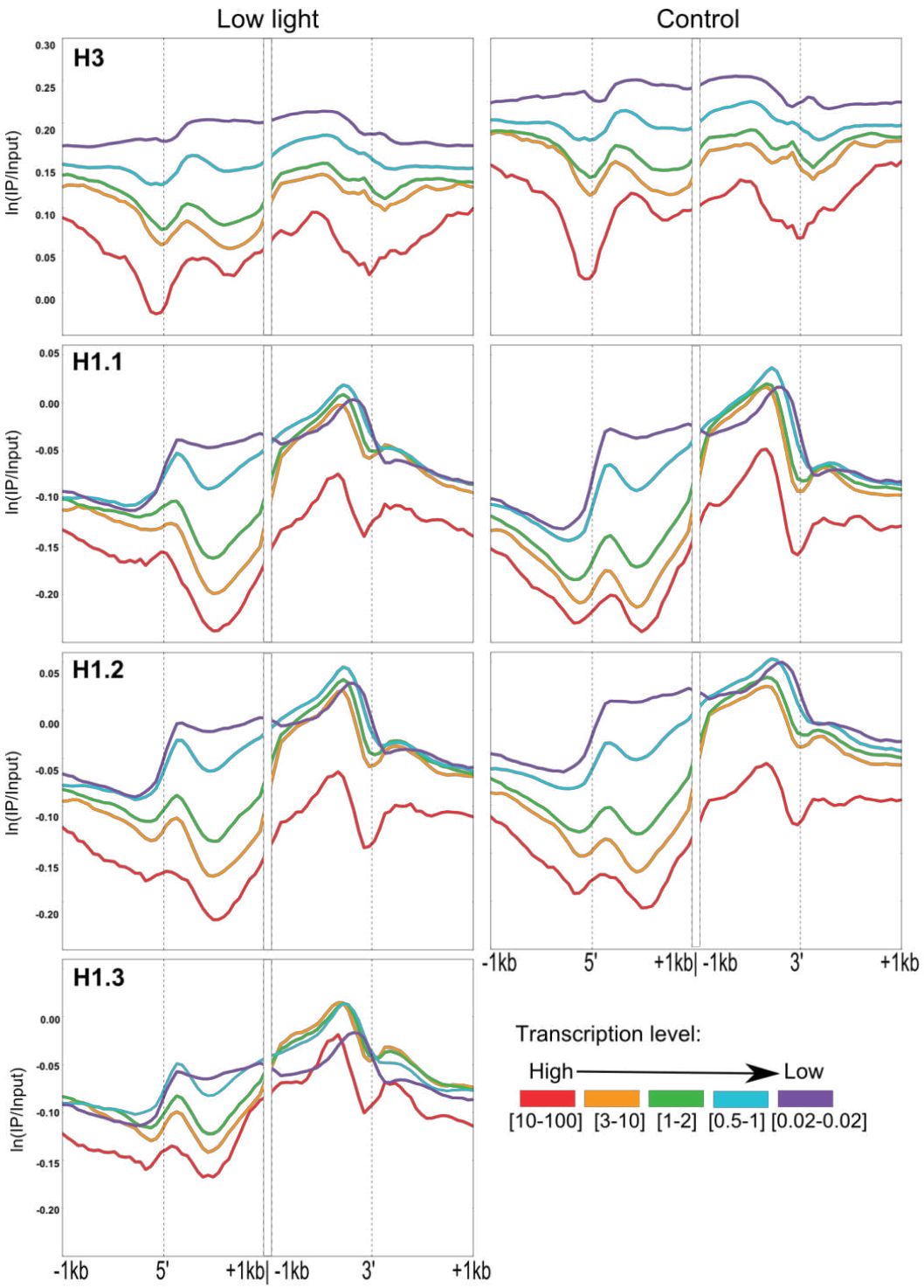

Figure 6. Distribution of H1s and H3 within genes according to their level of transcription in control conditions and low light.

The signal for histone occupancy was plotted for 1 kb around both the 5' (TSS) and 3' ends for five classes of genes divided according to their expression level.

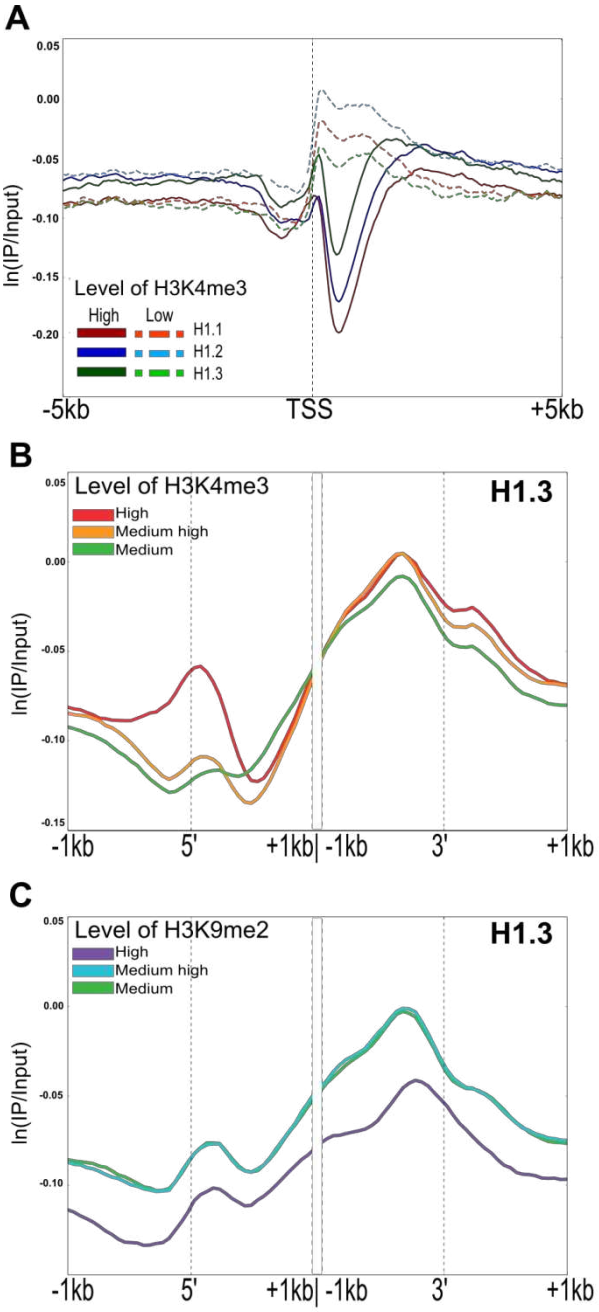

Figure 7. Occupancy of linker histone variants in the Arabidopsis genome.

(A) H1 occupancies in low light observed in 5 kb around the TSS for a group of 4495 genes with the highest and 5999 genes with the lowest level of H3K4me3. **(B)** H1.3 distribution among genes divided according to the level of H3K4me3. **(C)** H1.3 distribution among genes divided according to the level of H3K9me2.

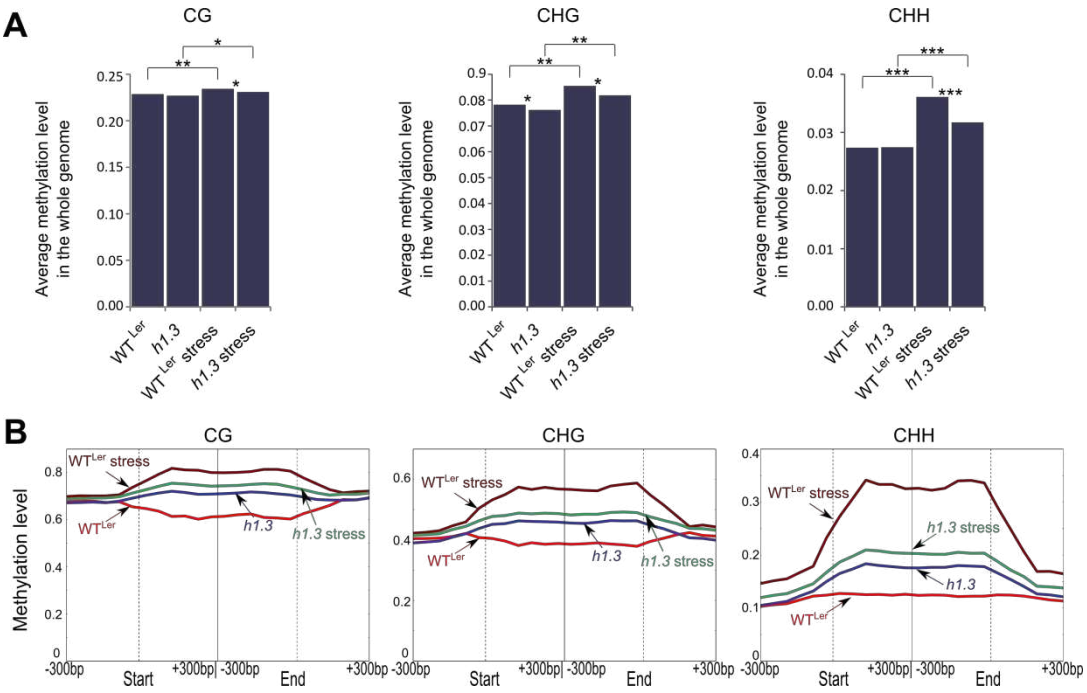

Figure 8. H1.3 is required for *de novo* DNA methylation in response to low light/drought.

(A) Averaged DNA methylation level in the CG, CHG and CHH contexts in wild-type (WT^{Ler}) and *h1.3* Arabidopsis in control and in low light/drought conditions (stress). Asterisks indicate level of significance: *** $p<10^{-256}$, ** $p<10^{-30}$, * $p<10^{-10}$ (T-test). **(B)** Patterns of DNA methylation (in the CG, CHG and CHH contexts) in regions that are hypermethylated in response to stress, for wild-type (WT^{Ler}) and *h1.3* plants in control and in low light/drought conditions. Averaged methylation (within a sliding 50-bp window) was plotted for 300 bp around both the start and the end of the regions.

Parsed Citations

ALTSCHUL, S. F., MADDEN, T. L., SCHAFFER, A. A., ZHANG, J., ZHANG, Z., MILLER, W. & LIPMAN, D. J. 1997. Gapped BLAST and PSI-BLAST: a new generation of protein database search programs. Nucleic Acids Res, 25, 3389-402.

Pubmed: Author and Title
CrossRef: Author and Title
Google Scholar: Author Only Title Only Author and Title

ANISIMOVA, M. & GASCUEL, O. 2006. Approximate likelihood-ratio test for branches: A fast, accurate, and powerful alternative. Syst Biol, 55, 539-52.

Pubmed: Author and Title
CrossRef: Author and Title
Google Scholar: Author Only Title Only Author and Title

ARABIDOPSIS GENOME, I. 2000. Analysis of the genome sequence of the flowering plant Arabidopsis thaliana. Nature, 408, 796-815.

Pubmed: Author and Title
CrossRef: Author and Title
Google Scholar: Author Only Title Only Author and Title

ASCENZI, R. & GANTT, J. S. 1997. A drought-stress-inducible histone gene in Arabidopsis thaliana is a member of a distinct class of plant linker histone variants. Plant Mol Biol, 34, 629-41.

Pubmed: Author and Title
CrossRef: Author and Title
Google Scholar: Author Only Title Only Author and Title

ASCENZI, R. & GANTT, J. S. 1999a. Molecular genetic analysis of the drought-inducible linker histone variant in Arabidopsis thaliana. Plant Mol Biol, 41, 159-69.

Pubmed: Author and Title
CrossRef: Author and Title
Google Scholar: Author Only Title Only Author and Title

ASCENZI, R. & GANTT, J. S. 1999b. Subnuclear distribution of the entire complement of linker histone variants in Arabidopsis thaliana. Chromosoma, 108, 345-55.

Pubmed: Author and Title
CrossRef: Author and Title
Google Scholar: Author Only Title Only Author and Title

BANAS, A. K., LABUZ, J., SZTATELMAN, O., GABRYS, H. & FIEDOR, L. 2011. Expression of enzymes involved in chlorophyll catabolism in Arabidopsis is light controlled. Plant Physiol, 157, 1497-504.

Pubmed: Author and Title
CrossRef: Author and Title
Google Scholar: Author Only Title Only Author and Title

BAUER, H., ACHE, P., LAUTNER, S., FROMM, J., HARTUNG, W., AL-RASHEID, K. A., SONNEWALD, S., SONNEWALD, U., KNEITZ, S., LACHMANN, N., MENDEL, R. R., BITTNER, F., HETHERINGTON, A. M. & HEDRICH, R. 2013. The stomatal response to reduced relative humidity requires guard cell-autonomous ABA synthesis. Curr Biol, 23, 53-7.

Pubmed: Author and Title
CrossRef: Author and Title
Google Scholar: Author Only Title Only Author and Title

BERENDZEN, S. M., CAREY, J. D. & SMITH, E. B. 2006. Diltiazem-associated photodistributed hyperpigmentation in an elderly Hispanic female. Int J Dermatol, 45, 1450-2.

Pubmed: Author and Title
CrossRef: Author and Title
Google Scholar: Author Only Title Only Author and Title

BILGER, W. & BJORKMAN, O. 1991. Temperature dependence of violaxanthin de-epoxidation and non-photochemical fluorescence quenching in intact leaves of Gossypium hirsutum L. and Malva parviflora L. Planta, 184, 226-34.

Pubmed: Author and Title
CrossRef: Author and Title
Google Scholar: Author Only Title Only Author and Title

BRAUNSCHWEIG, U., HOGAN, G. J., PAGIE, L. & VAN STEENSEL, B. 2009. Histone H1 binding is inhibited by histone variant H3.3. EMBO J, 28, 3635-45.

Pubmed: Author and Title
CrossRef: Author and Title
Google Scholar: Author Only Title Only Author and Title

BROWN, D. T., IZARD, T. & MISTELI, T. 2006. Mapping the interaction surface of linker histone H1(0) with the nucleosome of native chromatin in vivo. Nat Struct Mol Biol, 13, 250-5.

Pubmed: Author and Title
CrossRef: Author and Title
Google Scholar: Author Only Title Only Author and Title

BRZESKI, J. & JERZMANOWSKI, A. 2003. Deficient in DNA methylation 1 (DDM1) defines a novel family of chromatin-remodeling factors. J Biol Chem, 278, 823-8.

Pubmed: Author and Title
CrossRef: Author and Title

Google Scholar: Author Only Title Only Author and Title

CAO, K., LAILLER, N., ZHANG, Y., KUMAR, A., UPPAL, K., LIU, Z., LEE, E. K., WU, H., MEDRZYCKI, M., PAN, C., HO, P. Y., COOPER, G. P., JR., DONG, X., BOCK, C., BOUHASSIRA, E. E. & FAN, Y. 2013. High-resolution mapping of h1 linker histone variants in embryonic stem cells. PLoS Genet, 9, e1003417.

Pubmed: Author and Title
CrossRef: Author and Title
Google Scholar: Author Only Title Only Author and Title

CAPELLA-GUTIERREZ, S., SILLA-MARTINEZ, J. M. & GABALDON, T. 2009. trimAl: a tool for automated alignment trimming in large-scale phylogenetic analyses. Bioinformatics, 25, 1972-3.

Pubmed: Author and Title
CrossRef: Author and Title
Google Scholar: Author Only Title Only Author and Title

CATEZ, F., UEDA, T. & BUSTIN, M. 2006. Determinants of histone H1 mobility and chromatin binding in living cells. Nat Struct Mol Biol, 13, 305-10.

Pubmed: Author and Title
CrossRef: Author and Title
Google Scholar: Author Only Title Only Author and Title

CATEZ, F., YANG, H., TRACEY, K. J., REEVES, R., MISTELI, T. & BUSTIN, M. 2004. Network of dynamic interactions between histone H1 and high-mobility-group proteins in chromatin. Mol Cell Biol, 24, 4321-8.

Pubmed: Author and Title
CrossRef: Author and Title
Google Scholar: Author Only Title Only Author and Title

CHAVES, M. M., FLEXAS, J. & PINHEIRO, C. 2009. Photosynthesis under drought and salt stress: regulation mechanisms from whole plant to cell. Ann Bot, 103, 551-60.

Pubmed: Author and Title
CrossRef: Author and Title
Google Scholar: Author Only Title Only Author and Title

CHRISTOPHOROU, M. A., CASTELO-BRANCO, G., HALLEY-STOTT, R. P., OLIVEIRA, C. S., LOOS, R., RADZISHEUSKAYA, A., MOWEN, K. A., BERTONE, P., SILVA, J. C., ZERNICKA-GOETZ, M., NIELSEN, M. L., GURDON, J. B. & KOUZARIDES, T. 2014. Citrullination regulates pluripotency and histone H1 binding to chromatin. Nature, 507, 104-8.

Pubmed: Author and Title
CrossRef: Author and Title
Google Scholar: Author Only Title Only Author and Title

CLOUGH, S. J. & BENT, A. F. 1998. Floral dip: a simplified method for Agrobacterium-mediated transformation of Arabidopsis thaliana. Plant J, 16, 735-43.

Pubmed: Author and Title
CrossRef: Author and Title
Google Scholar: Author Only Title Only Author and Title

COHEN, A. & BRAY, E. A. 1990. Characterization of three mRNAs that accumulate in wilted tomato leaves in response to elevated levels of endogenous abscisic acid. Planta, 182, 27-33.

Pubmed: Author and Title
CrossRef: Author and Title
Google Scholar: Author Only Title Only Author and Title

COHEN, A., PLANT, A. L., MOSES, M. S. & BRAY, E. A. 1991. Organ-Specific and Environmentally Regulated Expression of Two Abscisic Acid-Induced Genes of Tomato : Nucleotide Sequence and Analysis of the Corresponding cDNAs. Plant Physiol, 97, 1367-74.

Pubmed: Author and Title
CrossRef: Author and Title
Google Scholar: Author Only Title Only Author and Title

COLANERI, A. C. & JONES, A. M. 2013. Genome-wide quantitative identification of DNA differentially methylated sites in Arabidopsis seedlings growing at different water potential. PLoS One, 8, e59878.

Pubmed: Author and Title
CrossRef: Author and Title
Google Scholar: Author Only Title Only Author and Title

CROOKS, G. E., HON, G., CHANDONIA, J. M. & BRENNER, S. E. 2004. WebLogo: a sequence logo generator. Genome Res, 14, 1188-90.

Pubmed: Author and Title
CrossRef: Author and Title
Google Scholar: Author Only Title Only Author and Title

DOHENY-ADAMS, T., HUNT, L., FRANKS, P. J., BEERLING, D. J. & GRAY, J. E. 2012. Genetic manipulation of stomatal density influences stomatal size, plant growth and tolerance to restricted water supply across a growth carbon dioxide gradient. Philos Trans R Soc Lond B Biol Sci, 367, 547-55.

Pubmed: Author and Title
CrossRef: Author and Title
Google Scholar: Author Only Title Only Author and Title

DU, Z., ZHOU, X., LING, Y., ZHANG, Z. & SU, Z. 2010. agriGO: a GO analysis toolkit for the agricultural community. Nucleic Acids Res, 38, W64-70.

Pubmed: Author and Title
CrossRef: Author and Title
Google Scholar: Author Only Title Only Author and Title

DUBAS, E., JANOWIAK, F., KRZEWSKA, M., HURA, T. & ZUR, I. 2013. Endogenous ABA concentration and cytoplasmic membrane fluidity in microspores of oilseed rape (Brassica napus L.) genotypes differing in responsiveness to androgenesis induction. Plant Cell Rep, 32, 1465-75.
Pubmed: Author and Title
CrossRef: Author and Title
Google Scholar: Author Only Title Only Author and Title

FAN, Y., NIKITINA, T., ZHAO, J., FLEURY, T. J., BHATTACHARYYA, R., BOUHASSIRA, E. E., STEIN, A., WOODCOCK, C. L. & SKOULTCHI, A. I. 2005. Histone H1 depletion in mammals alters global chromatin structure but causes specific changes in gene regulation. Cell, 123, 1199-212.
Pubmed: Author and Title
CrossRef: Author and Title
Google Scholar: Author Only Title Only Author and Title

FEY, V., WAGNER, R., BRAUTIGAM, K. & PFANNSCHMIDT, T. 2005. Photosynthetic redox control of nuclear gene expression. J Exp Bot, 56, 1491-8.
Pubmed: Author and Title
CrossRef: Author and Title
Google Scholar: Author Only Title Only Author and Title

FRICKEY, T. & LUPAS, A. 2004. CLANS: a Java application for visualizing protein families based on pairwise similarity. Bioinformatics, 20, 3702-4.
Pubmed: Author and Title
CrossRef: Author and Title
Google Scholar: Author Only Title Only Author and Title

FUJITA, Y., FUJITA, M., SHINOZAKI, K. & YAMAGUCHI-SHINOZAKI, K. 2011. ABA-mediated transcriptional regulation in response to osmotic stress in plants. J Plant Res, 124, 509-25.
Pubmed: Author and Title
CrossRef: Author and Title
Google Scholar: Author Only Title Only Author and Title

GENTY, B., BRIANTAIS, J.-M. & BAKER, N. R. 1989. The relationship between the quantum yield of photosynthetic electron transport and quenching of chlorophyll fluorescence. Biochimica et Biophysica Acta (BBA) - General Subjects, 990, 87-92.
Pubmed: Author and Title
CrossRef: Author and Title
Google Scholar: Author Only Title Only Author and Title

GINALSKI, K., ELOFSSON, A., FISCHER, D. & RYCHLEWSKI, L. 2003. 3D-Jury: a simple approach to improve protein structure predictions. Bioinformatics, 19, 1015-8.
Pubmed: Author and Title
CrossRef: Author and Title
Google Scholar: Author Only Title Only Author and Title

GINALSKI, K. & RYCHLEWSKI, L. 2003. Protein structure prediction of CASP5 comparative modeling and fold recognition targets using consensus alignment approach and 3D assessment. Proteins, 53 Suppl 6, 410-7.
Pubmed: Author and Title
CrossRef: Author and Title
Google Scholar: Author Only Title Only Author and Title

GINALSKI, K., VON GROTTHUSS, M., GRISHIN, N. V. & RYCHLEWSKI, L. 2004. Detecting distant homology with Meta-BASIC. Nucleic Acids Res, 32, W576-81.
Pubmed: Author and Title
CrossRef: Author and Title
Google Scholar: Author Only Title Only Author and Title

GLASSER, C., HABERER, G., FINKEMEIER, I., PFANNSCHMIDT, T., KLEINE, T., LEISTER, D., DIETZ, K. J., HAUSLER, R. E., GRIMM, B. & MAYER, K. F. 2014. Meta-analysis of retrograde signaling in Arabidopsis thaliana reveals a core module of genes embedded in complex cellular signaling networks. Mol Plant, 7, 1167-90.
Pubmed: Author and Title
CrossRef: Author and Title
Google Scholar: Author Only Title Only Author and Title

GOMEZ-PORRAS, J. L., RIANO-PACHON, D. M., DREYER, I., MAYER, J. E. & MUELLER-ROEBER, B. 2007. Genome-wide analysis of ABA-responsive elements ABRE and CE3 reveals divergent patterns in Arabidopsis and rice. BMC Genomics, 8, 260.
Pubmed: Author and Title
CrossRef: Author and Title
Google Scholar: Author Only Title Only Author and Title

GUINDON, S., DUFAYARD, J. F., LEFORT, V., ANISIMOVA, M., HORDIJK, W. & GASCUEL, O. 2010. New algorithms and methods to estimate maximum-likelihood phylogenies: assessing the performance of PhyML 3.0. Syst Biol, 59, 307-21.
Pubmed: Author and Title
CrossRef: Author and Title
Google Scholar: Author Only Title Only Author and Title

GUO, L., ZHOU, J., ELLING, A. A., CHARRON, J. B. & DENG, X. W. 2008. Histone modifications and expression of light-regulated

genes in Arabidopsis are cooperatively influenced by changing light conditions. Plant Physiol, 147, 2070-83.
Pubmed: Author and Title
CrossRef: Author and Title
Google Scholar: Author Only Title Only Author and Title

HARSHMAN, S. W., YOUNG, N. L., PARTHUN, M. R. & FREITAS, M. A. 2013. H1 histones: current perspectives and challenges. Nucleic Acids Res, 41, 9593-609.
Pubmed: Author and Title
CrossRef: Author and Title
Google Scholar: Author Only Title Only Author and Title

IZZO, A., KAMIENIARZ-GDULA, K., RAMIREZ, F., NOUREEN, N., KIND, J., MANKE, T., VAN STEENSEL, B. & SCHNEIDER, R. 2013. The genomic landscape of the somatic linker histone subtypes H1.1 to H1.5 in human cells. Cell Rep, 3, 2142-54.
Pubmed: Author and Title
CrossRef: Author and Title
Google Scholar: Author Only Title Only Author and Title

JEDDELOH, J. A., BENDER, J. & RICHARDS, E. J. 1998. The DNA methylation locus DDM1 is required for maintenance of gene silencing in Arabidopsis. Genes Dev, 12, 1714-25.
Pubmed: Author and Title
CrossRef: Author and Title
Google Scholar: Author Only Title Only Author and Title

JERZMANOWSKI, A., PRZEWLOKA, M. & GRASSER, K. D. 2000. Linker Histones and HMG1 Proteins of Higher Plants. Plant Biology, 2, 586-597.
Pubmed: Author and Title
CrossRef: Author and Title
Google Scholar: Author Only Title Only Author and Title

JIANG, C. & PUGH, B. F. 2009. Nucleosome positioning and gene regulation: advances through genomics. Nat Rev Genet, 10, 161-72.
Pubmed: Author and Title
CrossRef: Author and Title
Google Scholar: Author Only Title Only Author and Title

JIAO, Y., WICKETT, N. J., AYYAMPALAYAM, S., CHANDERBALI, A. S., LANDHERR, L., RALPH, P. E., TOMSHO, L. P., HU, Y., LIANG, H., SOLTIS, P. S., SOLTIS, D. E., CLIFTON, S. W., SCHLARBAUM, S. E., SCHUSTER, S. C., MA, H., LEEBENS-MACK, J. & DEPAMPHILIS, C. W. 2011. Ancestral polyploidy in seed plants and angiosperms. Nature, 473, 97-100.
Pubmed: Author and Title
CrossRef: Author and Title
Google Scholar: Author Only Title Only Author and Title

JULLIEN, J., ASTRAND, C., HALLEY-STOTT, R. P., GARRETT, N. & GURDON, J. B. 2010. Characterization of somatic cell nuclear reprogramming by oocytes in which a linker histone is required for pluripotency gene reactivation. Proc Natl Acad Sci U S A, 107, 5483-8.
Pubmed: Author and Title
CrossRef: Author and Title
Google Scholar: Author Only Title Only Author and Title

KATOH, K. & STANDLEY, D. M. 2013. MAFFT multiple sequence alignment software version 7: improvements in performance and usability. Mol Biol Evol, 30, 772-80.
Pubmed: Author and Title
CrossRef: Author and Title
Google Scholar: Author Only Title Only Author and Title

KHANDELWAL, A., ELVITIGALA, T., GHOSH, B. & QUATRANO, R. S. 2008. Arabidopsis transcriptome reveals control circuits regulating redox homeostasis and the role of an AP2 transcription factor. Plant Physiol, 148, 2050-8.
Pubmed: Author and Title
CrossRef: Author and Title
Google Scholar: Author Only Title Only Author and Title

KILIAN, J., WHITEHEAD, D., HORAK, J., WANKE, D., WEINL, S., BATISTIC, O., D'ANGELO, C., BORNBERG-BAUER, E., KUDLA, J. & HARTER, K. 2007. The AtGenExpress global stress expression data set: protocols, evaluation and model data analysis of UV-B light, drought and cold stress responses. Plant J, 50, 347-63.
Pubmed: Author and Title
CrossRef: Author and Title
Google Scholar: Author Only Title Only Author and Title

KINOSHITA, T. & SEKI, M. 2014. Epigenetic memory for stress response and adaptation in plants. Plant Cell Physiol, 55, 1859-63.
Pubmed: Author and Title
CrossRef: Author and Title
Google Scholar: Author Only Title Only Author and Title

KLEPPER, B. & BARRS, H. D. 1968. Effects of salt secretion on psychrometric determinations of water potential of cotton leaves. Plant Physiol, 43, 1138-40.
Pubmed: Author and Title
CrossRef: Author and Title
Google Scholar: Author Only Title Only Author and Title

KLUGHAMMER, C. & SCHREIBER, U. 1994. An improved method, using saturating light pulses, for the determination of

photosystem I quantum yield via P700+-absorbance changes at 830 nm. Planta, 192, 261-268.
Pubmed: Author and Title
CrossRef: Author and Title
Google Scholar: Author Only Title Only Author and Title

KRIVOV, G. G., SHAPOVALOV, M. V. & DUNBRACK, R. L., JR. 2009. Improved prediction of protein side-chain conformations with SCWRL4. Proteins, 77, 778-95.
Pubmed: Author and Title
CrossRef: Author and Title
Google Scholar: Author Only Title Only Author and Title

KRUEGER, F. & ANDREWS, S. R. 2011. Bismark: a flexible aligner and methylation caller for Bisulfite-Seq applications. Bioinformatics, 27, 1571-2.
Pubmed: Author and Title
CrossRef: Author and Title
Google Scholar: Author Only Title Only Author and Title

KUMARI, A., JEWARIA, P. K., BERGMANN, D. C. & KAKIMOTO, T. 2014. Arabidopsis reduces growth under osmotic stress by decreasing SPEECHLESS protein. Plant Cell Physiol, 55, 2037-46.
Pubmed: Author and Title
CrossRef: Author and Title
Google Scholar: Author Only Title Only Author and Title

LAKE, J. A., QUICK, W. P., BEERLING, D. J. & WOODWARD, F. I. 2001. Plant development. Signals from mature to new leaves. Nature, 411, 154.
Pubmed: Author and Title
CrossRef: Author and Title
Google Scholar: Author Only Title Only Author and Title

LAU, O. S. & BERGMANN, D. C. 2012. Stomatal development: a plant's perspective on cell polarity, cell fate transitions and intercellular communication. Development, 139, 3683-92.
Pubmed: Author and Title
CrossRef: Author and Title
Google Scholar: Author Only Title Only Author and Title

LAUNHOLT, D., MERKLE, T., HOUBEN, A., SCHULZ, A. & GRASSER, K. D. 2006. Arabidopsis chromatin-associated HMGA and HMGB use different nuclear targeting signals and display highly dynamic localization within the nucleus. Plant Cell, 18, 2904-18.
Pubmed: Author and Title
CrossRef: Author and Title
Google Scholar: Author Only Title Only Author and Title

LEONHARDT, N., KWAK, J. M., ROBERT, N., WANER, D., LEONHARDT, G. & SCHROEDER, J. I. 2004. Microarray expression analyses of Arabidopsis guard cells and isolation of a recessive abscisic acid hypersensitive protein phosphatase 2C mutant. Plant Cell, 16, 596-615.
Pubmed: Author and Title
CrossRef: Author and Title
Google Scholar: Author Only Title Only Author and Title

LEPISTO, A., TOIVOLA, J., NIKKANEN, L. & RINTAMAKI, E. 2012. Retrograde signaling from functionally heterogeneous plastids. Front Plant Sci, 3, 286.
Pubmed: Author and Title
CrossRef: Author and Title
Google Scholar: Author Only Title Only Author and Title

LETUNIC, I. & BORK, P. 2011. Interactive Tree Of Life v2: online annotation and display of phylogenetic trees made easy. Nucleic Acids Res, 39, W475-8.
Pubmed: Author and Title
CrossRef: Author and Title
Google Scholar: Author Only Title Only Author and Title

LETUNIC, I., COPLEY, R. R., PILS, B., PINKERT, S., SCHULTZ, J. & BORK, P. 2006. SMART 5: domains in the context of genomes and networks. Nucleic Acids Res, 34, D257-60.
Pubmed: Author and Title
CrossRef: Author and Title
Google Scholar: Author Only Title Only Author and Title

LIPPMAN, Z., GENDREL, A. V., BLACK, M., VAUGHN, M. W., DEDHIA, N., MCCOMBIE, W. R., LAVINE, K., MITTAL, V., MAY, B., KASSCHAU, K. D., CARRINGTON, J. C., DOERGE, R. W., COLOT, V. & MARTIENSSEN, R. 2004. Role of transposable elements in heterochromatin and epigenetic control. Nature, 430, 471-6.
Pubmed: Author and Title
CrossRef: Author and Title
Google Scholar: Author Only Title Only Author and Title

LUO, C., SIDOTE, D. J., ZHANG, Y., KERSTETTER, R. A., MICHAEL, T. P. & LAM, E. 2012. Integrative analysis of chromatin states in Arabidopsis identified potential regulatory mechanisms for natural antisense transcript production. Plant J.
Pubmed: Author and Title
CrossRef: Author and Title
Google Scholar: Author Only Title Only Author and Title

LUPAS, A., VAN DYKE, M. & STOCK, J. 1991. Predicting coiled coils from protein sequences. Science, 252, 1162-4.

Pubmed: Author and Title
CrossRef: Author and Title
Google Scholar: Author Only Title Only Author and Title

MACALISTER, C. A., OHASHI-ITO, K. & BERGMANN, D. C. 2007. Transcription factor control of asymmetric cell divisions that establish the stomatal lineage. Nature, 445, 537-40.
Pubmed: Author and Title
CrossRef: Author and Title
Google Scholar: Author Only Title Only Author and Title

MARCHLER-BAUER, A., LU, S., ANDERSON, J. B., CHITSAZ, F., DERBYSHIRE, M. K., DEWEESE-SCOTT, C., FONG, J. H., GEER, L. Y., GEER, R. C., GONZALES, N. R., GWADZ, M., HURWITZ, D. I., JACKSON, J. D., KE, Z., LANCZYCKI, C. J., LU, F., MARCHLER, G. H., MULLOKANDOV, M., OMELCHENKO, M. V., ROBERTSON, C. L., SONG, J. S., THANKI, N., YAMASHITA, R. A., ZHANG, D., ZHANG, N., ZHENG, C. & BRYANT, S. H. 2011. CDD: a Conserved Domain Database for the functional annotation of proteins. Nucleic Acids Res, 39, D225-9.
Pubmed: Author and Title
CrossRef: Author and Title
Google Scholar: Author Only Title Only Author and Title

MCBRYANT, S. J., LU, X. & HANSEN, J. C. 2010. Multifunctionality of the linker histones: an emerging role for protein-protein interactions. Cell Res, 20, 519-28.
Pubmed: Author and Title
CrossRef: Author and Title
Google Scholar: Author Only Title Only Author and Title

MOISSIARD, G., COKUS, S. J., CARY, J., FENG, S., BILLI, A. C., STROUD, H., HUSMANN, D., ZHAN, Y., LAJOIE, B. R., MCCORD, R. P., HALE, C. J., FENG, W., MICHAELS, S. D., FRAND, A. R., PELLEGRINI, M., DEKKER, J., KIM, J. K. & JACOBSEN, S. E. 2012. MORC family ATPases required for heterochromatin condensation and gene silencing. Science, 336, 1448-51.
Pubmed: Author and Title
CrossRef: Author and Title
Google Scholar: Author Only Title Only Author and Title

MOTT, R. 2000. Accurate formula for P-values of gapped local sequence and profile alignments. J Mol Biol, 300, 649-59.
Pubmed: Author and Title
CrossRef: Author and Title
Google Scholar: Author Only Title Only Author and Title

NEDBAL L., W., J. 2004. Chlorophyll fluorescence imaging of leaves and fruits. Papageorgiou, G., Govindjee, editors. Chlorophyll fluorescence, a signature of photosynthesis, Dordrecht Springer, 389-407.
Pubmed: Author and Title
CrossRef: Author and Title
Google Scholar: Author Only Title Only Author and Title

NELSON, J. D., DENISENKO, O., SOVA, P. & BOMSZTYK, K. 2006. Fast chromatin immunoprecipitation assay. Nucleic Acids Res, 34, e2.
Pubmed: Author and Title
CrossRef: Author and Title
Google Scholar: Author Only Title Only Author and Title

NIELSEN, H., ENGELBRECHT, J., BRUNAK, S. & VON HEIJNE, G. 1997. Identification of prokaryotic and eukaryotic signal peptides and prediction of their cleavage sites. Protein Eng, 10, 1-6.
Pubmed: Author and Title
CrossRef: Author and Title
Google Scholar: Author Only Title Only Author and Title

PARKINSON, K. J., DAY, W. & LEACH, J. E. 1980. A Portable System for Measuring the Photosynthesis and Transpiration of Graminaceous Leaves. Journal of Experimental Botany, 31, 1441-1453.
Pubmed: Author and Title
CrossRef: Author and Title
Google Scholar: Author Only Title Only Author and Title

PEI, J., SADREYEV, R. & GRISHIN, N. V. 2003. PCMA: fast and accurate multiple sequence alignment based on profile consistency. Bioinformatics, 19, 427-8.
Pubmed: Author and Title
CrossRef: Author and Title
Google Scholar: Author Only Title Only Author and Title

PEREZ-MONTERO, S., CARBONELL, A., MORAN, T., VAQUERO, A. & AZORIN, F. 2013. The embryonic linker histone H1 variant of Drosophila, dBigH1, regulates zygotic genome activation. Dev Cell, 26, 578-90.
Pubmed: Author and Title
CrossRef: Author and Title
Google Scholar: Author Only Title Only Author and Title

PFALZ, J., LIEBERS, M., HIRTH, M., GRUBLER, B., HOLTZEGEL, U., SCHROTER, Y., DIETZEL, L. & PFANNSCHMIDT, T. 2012. Environmental control of plant nuclear gene expression by chloroplast redox signals. Front Plant Sci, 3, 257.
Pubmed: Author and Title
CrossRef: Author and Title
Google Scholar: Author Only Title Only Author and Title

PHAIR, R. D., SCAFFIDI, P., ELBI, C., VECEROVA, J., DEY, A., OZATO, K., BROWN, D. T., HAGER, G., BUSTIN, M. & MISTELI, T.

2004. Global nature of dynamic protein-chromatin interactions in vivo: three-dimensional genome scanning and dynamic interaction networks of chromatin proteins. Mol Cell Biol, 24, 6393-402.
Pubmed: Author and Title
CrossRef: Author and Title
Google Scholar: Author Only Title Only Author and Title

PLANT, A. L., COHEN, A., MOSES, M. S. & BRAY, E. A. 1991. Nucleotide sequence and spatial expression pattern of a drought- and abscisic Acid-induced gene of tomato. Plant Physiol, 97, 900-6.
Pubmed: Author and Title
CrossRef: Author and Title
Google Scholar: Author Only Title Only Author and Title

PRZEWLOKA, M. R., WIERZBICKI, A. T., SLUSARCZYK, J., KURAS, M., GRASSER, K. D., STEMMER, C. & JERZMANOWSKI, A. 2002. The "drought-inducible" histone H1s of tobacco play no role in male sterility linked to alterations in H1 variants. Planta, 215, 371-9.
Pubmed: Author and Title
CrossRef: Author and Title
Google Scholar: Author Only Title Only Author and Title

RAGHURAM, N., CARRERO, G., TH'NG, J. & HENDZEL, M. J. 2009. Molecular dynamics of histone H1. Biochem Cell Biol, 87, 189-206.
Pubmed: Author and Title
CrossRef: Author and Title
Google Scholar: Author Only Title Only Author and Title

RAMAKRISHNAN, V., FINCH, J. T., GRAZIANO, V., LEE, P. L. & SWEET, R. M. 1993. Crystal structure of globular domain of histone H5 and its implications for nucleosome binding. Nature, 362, 219-23.
Pubmed: Author and Title
CrossRef: Author and Title
Google Scholar: Author Only Title Only Author and Title

REA, M., ZHENG, W., CHEN, M., BRAUD, C., BHANGU, D., ROGNAN, T. N. & XIAO, W. 2012. Histone H1 affects gene imprinting and DNA methylation in Arabidopsis. Plant J, 71, 776-86.
Pubmed: Author and Title
CrossRef: Author and Title
Google Scholar: Author Only Title Only Author and Title

REHRAUER, H., AQUINO, C., GRUISSEM, W., HENZ, S. R., HILSON, P., LAUBINGER, S., NAOUAR, N., PATRIGNANI, A., ROMBAUTS, S., SHU, H., VAN DE PEER, Y., VUYLSTEKE, M., WEIGEL, D., ZELLER, G. & HENNIG, L. 2010. AGRONOMICS1: a new resource for Arabidopsis transcriptome profiling. Plant Physiol, 152, 487-99.
Pubmed: Author and Title
CrossRef: Author and Title
Google Scholar: Author Only Title Only Author and Title

ROSA, S., NTOUKAKIS, V., OHMIDO, N., PENDLE, A., ABRANCHES, R. & SHAW, P. 2014. Cell differentiation and development in Arabidopsis are associated with changes in histone dynamics at the single-cell level. Plant Cell, 26, 4821-33.
Pubmed: Author and Title
CrossRef: Author and Title
Google Scholar: Author Only Title Only Author and Title

SALI, A. & BLUNDELL, T. L. 1993. Comparative protein modelling by satisfaction of spatial restraints. J Mol Biol, 234, 779-815.
Pubmed: Author and Title
CrossRef: Author and Title
Google Scholar: Author Only Title Only Author and Title

SCHMID, M., DAVISON, T. S., HENZ, S. R., PAPE, U. J., DEMAR, M., VINGRON, M., SCHOLKOPF, B., WEIGEL, D. & LOHMANN, J. U. 2005. A gene expression map of Arabidopsis thaliana development. Nat Genet, 37, 501-6.
Pubmed: Author and Title
CrossRef: Author and Title
Google Scholar: Author Only Title Only Author and Title

SCIPPA, G. S., DI MICHELE, M., ONELLI, E., PATRIGNANI, G., CHIATANTE, D. & BRAY, E. A. 2004. The histone-like protein H1-S and the response of tomato leaves to water deficit. J Exp Bot, 55, 99-109.
Pubmed: Author and Title
CrossRef: Author and Title
Google Scholar: Author Only Title Only Author and Title

SCIPPA, G. S., GRIFFITHS, A., CHIATANTE, D. & BRAY, E. A. 2000. The H1 histone variant of tomato, H1-S, is targeted to the nucleus and accumulates in chromatin in response to water-deficit stress. Planta, 211, 173-81.
Pubmed: Author and Title
CrossRef: Author and Title
Google Scholar: Author Only Title Only Author and Title

SHAHHOSEINI, M., FAVAEDI, R., BAHARVAND, H., SHARMA, V. & STUNNENBERG, H. G. 2010. Evidence for a dynamic role of the linker histone variant H1x during retinoic acid-induced differentiation of NT2 cells. FEBS Lett, 584, 4661-4.
Pubmed: Author and Title
CrossRef: Author and Title
Google Scholar: Author Only Title Only Author and Title

SHE, W., GRIMANELLI, D., RUTOWICZ, K., WHITEHEAD, M. W., PUZIO, M., KOTLINSKI, M., JERZMANOWSKI, A. & BAROUX, C. 2013. Chromatin reprogramming during the somatic-to-reproductive cell fate transition in plants. Development, 140, 4008-19.

Pubmed: Author and Title
CrossRef: Author and Title
Google Scholar: Author Only Title Only Author and Title

SMITH, K. T. & WORKMAN, J. L. 2012. Chromatin proteins: key responders to stress. PLoS Biol, 10, e1001371.
Pubmed: Author and Title
CrossRef: Author and Title
Google Scholar: Author Only Title Only Author and Title

STASEVICH, T. J., MUELLER, F., BROWN, D. T. & MCNALLY, J. G. 2010. Dissecting the binding mechanism of the linker histone in live cells: an integrated FRAP analysis. EMBO J, 29, 1225-34.
Pubmed: Author and Title
CrossRef: Author and Title
Google Scholar: Author Only Title Only Author and Title

STRIZHOV, N., ABRAHAM, E., OKRESZ, L., BLICKLING, S., ZILBERSTEIN, A., SCHELL, J., KONCZ, C. & SZABADOS, L. 1997. Differential expression of two P5CS genes controlling proline accumulation during salt-stress requires ABA and is regulated by ABA1, ABI1 and AXR2 in Arabidopsis. Plant J, 12, 557-69.
Pubmed: Author and Title
CrossRef: Author and Title
Google Scholar: Author Only Title Only Author and Title

TALBERT, P. B., AHMAD, K., ALMOUZNI, G., AUSIO, J., BERGER, F., BHALLA, P. L., BONNER, W. M., CANDE, W. Z., CHADWICK, B. P., CHAN, S. W., CROSS, G. A., CUI, L., DIMITROV, S. I., DOENECKE, D., EIRIN-LOPEZ, J. M., GOROVSKY, M. A., HAKE, S. B., HAMKALO, B. A., HOLEC, S., JACOBSEN, S. E., KAMIENIARZ, K., KHOCHBIN, S., LADURNER, A. G., LANDSMAN, D., LATHAM, J. A., LOPPIN, B., MALIK, H. S., MARZLUFF, W. F., PEHRSON, J. R., POSTBERG, J., SCHNEIDER, R., SINGH, M. B., SMITH, M. M., THOMPSON, E., TORRES-PADILLA, M. E., TREMETHICK, D. J., TURNER, B. M., WATERBORG, J. H., WOLLMANN, H., YELAGANDULA, R., ZHU, B. & HENIKOFF, S. 2012. A unified phylogeny-based nomenclature for histone variants. Epigenetics Chromatin, 5, 7.
Pubmed: Author and Title
CrossRef: Author and Title
Google Scholar: Author Only Title Only Author and Title

VAN DIJK, K., DING, Y., MALKARAM, S., RIETHOVEN, J. J., LIU, R., YANG, J., LACZKO, P., CHEN, H., XIA, Y., LADUNGA, I., AVRAMOVA, Z. & FROMM, M. 2010. Dynamic changes in genome-wide histone H3 lysine 4 methylation patterns in response to dehydration stress in Arabidopsis thaliana. BMC Plant Biol, 10, 238.
Pubmed: Author and Title
CrossRef: Author and Title
Google Scholar: Author Only Title Only Author and Title

VAN ZANTEN, M., TESSADORI, F., MCLOUGHLIN, F., SMITH, R., MILLENAAR, F. F., VAN DRIEL, R., VOESENEK, L. A., PEETERS, A. J. & FRANSZ, P. 2010. Photoreceptors CRYTOCHROME2 and phytochrome B control chromatin compaction in Arabidopsis. Plant Physiol, 154, 1686-96.
Pubmed: Author and Title
CrossRef: Author and Title
Google Scholar: Author Only Title Only Author and Title

WEI, T. & O'CONNELL, M. A. 1996. Structure and characterization of a putative drought-inducible H1 histone gene. Plant Mol Biol, 30, 255-68.
Pubmed: Author and Title
CrossRef: Author and Title
Google Scholar: Author Only Title Only Author and Title

WIERZBICKI, A. T. & JERZMANOWSKI, A. 2005. Suppression of histone H1 genes in Arabidopsis results in heritable developmental defects and stochastic changes in DNA methylation. Genetics, 169, 997-1008.
Pubmed: Author and Title
CrossRef: Author and Title
Google Scholar: Author Only Title Only Author and Title

WOOTTON, J. C. 1994. Non-globular domains in protein sequences: automated segmentation using complexity measures. Comput Chem, 18, 269-85.
Pubmed: Author and Title
CrossRef: Author and Title
Google Scholar: Author Only Title Only Author and Title

YANG, S. M., KIM, B. J., NORWOOD TORO, L. & SKOULTCHI, A. I. 2013. H1 linker histone promotes epigenetic silencing by regulating both DNA methylation and histone H3 methylation. Proc Natl Acad Sci U S A, 110, 1708-13.
Pubmed: Author and Title
CrossRef: Author and Title
Google Scholar: Author Only Title Only Author and Title

ZEMACH, A., KIM, M. Y., HSIEH, P. H., COLEMAN-DERR, D., ESHED-WILLIAMS, L., THAO, K., HARMER, S. L. & ZILBERMAN, D. 2013. The Arabidopsis nucleosome remodeler DDM1 allows DNA methyltransferases to access H1-containing heterochromatin. Cell, 153, 193-205.
Pubmed: Author and Title
CrossRef: Author and Title
Google Scholar: Author Only Title Only Author and Title

ZHANG, Y., COOKE, M., PANJWANI, S., CAO, K., KRAUTH, B., HO, P. Y., MEDRZYCKI, M., BERHE, D. T., PAN, C., MCDEVITT, T. C. & FAN, Y. 2012a. Histone h1 depletion impairs embryonic stem cell differentiation. PLoS Genet, 8, e1002691.

Pubmed: Author and Title
CrossRef: Author and Title
Google Scholar: Author Only Title Only Author and Title

ZHANG, Z., LI, J., ZHAO, X. Q., WANG, J., WONG, G. K. & YU, J. 2006. KaKs_Calculator: calculating Ka and Ks through model selection and model averaging. Genomics Proteomics Bioinformatics, 4, 259-63.

Pubmed: Author and Title
CrossRef: Author and Title
Google Scholar: Author Only Title Only Author and Title

ZHANG, Z., XIAO, J., WU, J., ZHANG, H., LIU, G., WANG, X. & DAI, L. 2012b. ParaAT: a parallel tool for constructing multiple protein-coding DNA alignments. Biochem Biophys Res Commun, 419, 779-81.

Pubmed: Author and Title
CrossRef: Author and Title
Google Scholar: Author Only Title Only Author and Title

ZHOU, J., WANG, X., HE, K., CHARRON, J. B., ELLING, A. A. & DENG, X. W. 2010. Genome-wide profiling of histone H3 lysine 9 acetylation and dimethylation in Arabidopsis reveals correlation between multiple histone marks and gene expression. Plant Mol Biol, 72, 585-95.

Pubmed: Author and Title
CrossRef: Author and Title
Google Scholar: Author Only Title Only Author and Title

ZIMMERMANN, P., HIRSCH-HOFFMANN, M., HENNIG, L. & GRUISSEM, W. 2004. GENEVESTIGATOR. Arabidopsis microarray database and analysis toolbox. Plant Physiol, 136, 2621-32.

Pubmed: Author and Title
CrossRef: Author and Title
Google Scholar: Author Only Title Only Author and Title

ZONG, W., ZHONG, X., YOU, J. & XIONG, L. 2013. Genome-wide profiling of histone H3K4-tri-methylation and gene expression in rice under drought stress. Plant Mol Biol, 81, 175-88.

Pubmed: Author and Title
CrossRef: Author and Title
Google Scholar: Author Only Title Only Author and Title